

1 ***The molecular interplay of the establishment of an infection – gene expression of***
2 ***Diaphorina citri* gut and *Candidatus Liberibacter asiaticus***

3

4 Flavia de Moura Manoel Bento¹; Josiane Cecília Darolt^{2,3}; Bruna Laís Merlin¹; Leandro
5 Penã^{2,4}; Nelson Arno Wulff^{2,3}; Fernando Luis Cônsoli¹

6

7 ¹Insect Interactions Laboratory, Department of Entomology and Acarology, Luiz de Queiroz
8 College of Agriculture, University of São Paulo, Piracicaba, São Paulo, Brazil.

9 ²Fund for Citrus Protection (FUNDECITRUS), 14807-040, Araraquara, São Paulo, Brazil.

10 ³Institute of Chemistry, São Paulo State University – UNESP, Araraquara, São Paulo, Brazil

11 ⁴Instituto de Biología Molecular y Celular de Plantas (IBMCP), Consejo Superior de
12 Investigaciones Científicas (CSIC), Universidad Politécnica de Valencia (UPV), 46022,
13 Valencia, Spain

14 Bento, F.M.M. – 0000-0003-1034-8943 - e-mail: flaviammbento@usp.br

15 Darolt, J.C. – ORCID: 0000-0003-3091-8747 -e-mail: josicdarolt@gmail.com:

16 Merlin, B.L. – ORCID: 0000-0003-4444-3906 - e-mail: bruna.merlin@usp.br

17 Penã, L. – ORCID: 0000-0002-9853-366X - e-mail: lpenya@fundecitrus.com.br;

18 lpenya@ibmcp.upv.es

19 Wulff, N.A. –ORCID:0000-0002-4557-2075 - e-mail: nelson.wulff@fundecitrus.com.br

20

21
22 **Corresponding author:**

23 **Fernando Luis Cônsoli: fconsoli@usp.br**

24 Insect Interactions Laboratory, Department of Entomology and Acarology, Luiz de Queiroz
25 College of Agriculture, University of São Paulo, Avenida Pádua Dias 11, 13418-900 Piracicaba,
26 São Paulo, Brazil.

27 **Abstract (max 300 words)**

28 *Candidatus Liberibacter asiaticus* (CLas) is one the causative agents of greening
29 disease in citrus, an uncurable, devastating disease of citrus worldwide. CLas is
30 vectored by *Diaphorina citri*, and the understanding of the molecular interplay between
31 vector and pathogen will provide additional basis for the development and
32 implementation of successful management strategies. We focused in the molecular
33 interplay occurring in the gut of the vector, a major barrier for CLas invasion and
34 colonization. We investigated the differential expression of vector and CLas genes by
35 analyzing a *de novo* reference metatranscriptome of the gut of adult psyllids fed of
36 CLas-infected and healthy citrus plants for 1-2, 3-4 and 5-6 days. CLas regulates the
37 immune response of the vector affecting the production of reactive species of oxygen
38 and nitrogen, and the production of antimicrobial peptides. Moreover, CLas
39 overexpressed *peroxiredoxin* in a protective manner. The major transcript involved in
40 immune expression was related to melanization, a *CLIP-domain serine protease* we
41 believe participates in the wounding of epithelial cells damaged during infection, which
42 is supported by the down-regulation of *pangolin*. We also detected that CLas modulates
43 the gut peristalsis of psyllids through the down-regulation of *titin*, reducing the
44 elimination of CLas with faeces. The up-regulation of the neuromodulator
45 *arylalkylamine N-acetyltransferase* implies CLas also interferes with the double brain-
46 gut communication circuitry of the vector. CLas colonizes the gut by expressing two
47 *Type IVb pilin flp* genes and several chaperones that can also function as adhesins. We
48 hypothesized biofil formation occurs by the expression of the cold shock protein of
49 CLas. We also describe the interplay during cell invasion and modification, and propose
50 mechanisms CLas uses to invade the host hemocel. We identified several specific
51 targets for the development of strategies directed to interfere with the successful
52 utilization of the psyllid vector by this pathogen.

53

54 **Keywords:** host regulation, effector proteins, host – pathogen interactions, pathogen's
55 ecology, infection strategies, host response to infection

57 **Author Summary**

58 Huanglongbing (HLB) or greening is an incurable disease causing severe damage to
59 citrus production, making citrus industrial activity unsustainable in several countries
60 around the world. HLB is caused by three species of *Candidatus* Liberibacter. *Ca.* L.
61 *asiaticus* (CLas), vectored by the psyllid *Diaphorina citri*, is the prevalent species.
62 Attempts to apply new technologies in the development of strategies for disease and
63 pest management are been made. However, we still miss basic information on this
64 system to efficiently apply the current technologies and envisage the implementation of
65 new approaches for pest control, despite the relevant scientific contribution available.
66 One major gap is regarded to the molecular interplay between CLas and its vector. We
67 focused our attention in the molecular interplay occurring at the first relevant interaction
68 of CLas and *D. citri*, represented by the gut barrier. We report the transcriptional
69 activity of CLas during the invasion and establishment of the infection in the gut of the
70 vector, as well as the transcriptional activity of the vector in response to the infection.
71 We identified several host genes that are targeted and regulated by CLas as well as
72 several CLas genes that are promising targets for the application of new management
73 strategies.

74

76 **1. Introduction**

77 Microbes often establish different interactions with metazoans depending on the
78 evolutionary history shared with their hosts. There are several examples of beneficial
79 associations with multicellular hosts resulting from distinct ecological interactions with
80 their hosts and associated trophic levels. But a concurrent number of interactions are
81 also known to be noxious to multicellular hosts due to the development of a range of
82 pathologies (Baumann 2005, Webb et al. 2006, Mansfield et al. 2012, Quigley 2013, Lu
83 et al. 2020)

84 Viruses are certainly the most common microbes infecting prokaryotes and
85 eukaryotes (Fauci 2001, Weinbauer 2004), and the year long pandemics caused by the
86 Sars-CoV2 virus is overshadowing other threatening pathogens to animals and plants.
87 Bacteria are widely associated with multicellular organisms, causing devastating
88 diseases. Bacteria-causing diseases in agricultural systems are a risk to food security,
89 causing severe losses in animal and plant production (Mansfield et al. 2012, Abebe et al.
90 2020).

91 Bacterial plant pathogens are also adapted to infect and propagate in insect
92 tissues, as many insects are used as vectors by plant pathogens to infect new host plants
93 and spread themselves in the environment. Plant pathogenic bacteria vectored by insects
94 that use persistent, circulative, propagative mode of transmission require plastic
95 phenotypes to interact with the different environments represented by sieves and tissues
96 of the host plant, and the diverse environments faced in the gut lumen, hemocele and
97 different tissues of the vector insect during the processes of acquisition and vector
98 competence development (Huang et al. 2020). The capability of these pathogens to
99 infect completely different hosts (plant and insect), and yet to depend on the shuttle host
100 (insect) to locate and collect the pathogen in a diseased plant, and later transport it to

101 new, healthy host plants for the establishment of new infections requires a set of
102 strategies devoted to manipulate the host insect (Perilla-Henao & Casteel 2016, Mauck
103 et al. 2018). The understanding of the interactions pathogens and hosts have at their
104 molecular level during the processes of host invasion and infection establishment is
105 required for a fully comprehension of the mechanisms involved in guaranteeing the host
106 – pathogen association. Such mechanisms of close interactions in the associations of
107 host and pathogens represent potential new targets for the development of new
108 technologies and/or use of existing technologies to interfere with the successful
109 association pathogens establish with their hosts.

110 *Candidatus* Liberibacter are bacteria posing serious threat to food security
111 worldwide by causing diseases to potatoes and citrus. Citrus is certainly the most
112 severely damaged crop by *Ca.* Liberibacter infections, as three different species are
113 known to infect citrus plants (*Ca.* L. asiaticus, *Ca.* L. americanus and *Ca.* L. africanus),
114 causing the incurable greening or huanglongbing (HLB) disease (Bové, 2006; Graça et
115 al., 2016; Tomaseto et al., 2019; Bassanezi et al., 2020). *Candidatus* Liberibacter did not
116 make to the top 10 plant pathogenic bacteria (Masnfield et al. 2012), but HLB has
117 caused a tremendous impact in the citrus industry and led to the complete elimination of
118 citrus orchards and the interruption of citrus production in what used to be highly
119 productive citrus centers (Dala-Paula et al. 2019, Bassanezi et al. 2020, Singerman &
120 Rogers 2020).

121 *Candidatus* Liberibacter asiaticus (CLas) is the most spread in the world,
122 currently infecting citrus in the major producing areas (CABI/EPPO 2017, Ajene et al.
123 2020, Wulff et al. 2020). In plants, *Candidatus* Liberibacter reside exclusively in the
124 phloem sieve tubes (Jagoueix et al., 1994; Bové & Garnier, 2003; Bové, 2006; Bendix
125 & Lewis, 2018), but it will infect several tissues of their host vector insect (Ammar et

126 al., 2011a; Ammar et al., 2017; Kruse et al., 2017; Ammar et al., 2019). CLas is
127 vectored by the worldwide distributed Asian Citrus Psyllid (ACP) *Diaphorina citri*
128 Kuwayama (Hemiptera: Liviidae) (Bové, 2006).

129 Despite the importance of this disease to the worldwide citriculture and all of the
130 investments and efforts of the scientific community to understand the interactions of the
131 pathogen with its vector, much of the mechanisms involved in the pathogen-vector
132 interplay remain unknown. We learned that CLas is transmitted from host plant to host
133 plant by establishing a persistent, propagative transmission mode with its vector, a
134 transmission mode that is very common to plant viruses vectored by aphids and
135 whiteflies (Gray et al., 2014; Ammar et al., 2016; Kruse et al., 2017). We also learned
136 CLas infects salivary glands and the midgut of vectors, tissues that are often recognized
137 as natural barriers to circulative, propagative pathogens as they can prevent
138 translocation of pathogens within the vector host (Ammar et al., 2011 a; Ammar et al.,
139 2011 b; Ammar et al., 2016; Ammar et al., 2020). More recently, new information on
140 the higher efficiency of adults than psyllid nymphs as vectors of CLas has been
141 reported, with adults displaying a higher successful rate of infection of healthy citrus
142 plants than nymphs (Ammar et al. 2020). Nevertheless, little information at the
143 physiological and molecular level on the interface of the interactions of CLas with key
144 vector tissues is available (Molki et al., 2019).

145 The limitations in the availability of efficient, cost-effective strategies for the
146 management of the vector and the disease prompted a large number of investigations for
147 the exploitation of new technologies, and promising results were mainly obtained with
148 RNAi-based approaches (Santos-Ortega & Killiny, 2018; Lu et al., 2019a; Lu et al.,
149 2019b; Yu & Killiny, 2020).

150 In here we focused on investigating the metatranscriptome of the gut of adults of
151 *D. citri* feeding on CLas-infected citrus plants for different periods of time in order to
152 identify genes of CLas that are expressed during the colonization of the gut of adults
153 and the differential gene expression in the gut of psyllids over time against psyllids
154 feeding on healthy, CLas-free citrus plants. Our major goal was to understand the
155 dynamics of CLas gene expression during psyllid colonization and the response
156 mechanisms that were activated in the gut epithelium of psyllids when exposed to *Ca.*
157 *Liberibacter asiaticus* cells. We believe our data represents a source of very specific
158 targets for the development and implementation of new strategies of psyllid/disease
159 control using RNAi and/or gene editing technologies such as the CRISPR-Cas9 system.

160

161 **2. Results**

162 **2.1. *De novo* transcriptome assembly**

163 Sequencing from libraries of the gut of uninfected and CLas-infected nymphs
164 and adults of *D. citri* yielded 395,151,161 reads, with an average of 16,464,632
165 reads/library. The use of the resulting 385,677,949 trimmed, quality-filtered reads
166 (average 16,069,915 reads/library) allowed the *de novo* assembly of a transcriptome
167 with 260,612,776 nucleotides (260 Mb), with transcripts with an average size of 481 bp
168 and a N50 of 2,095 bp. The assembly resulted in 248,850 transcripts with an average of
169 39.9% GC content. Annotation of the transcriptome allowed the putative identification
170 of 90,531 transcripts (36.4%), of which 52,081 transcripts were allocated to different
171 gene ontology categories (S1 Fig). Additional filtering using the highest score hit after
172 BlastX allowed the identification of 66,993 transcripts belonging to *D. citri*, 807
173 belonging to *Ca. Liberibacter*, and 1967 to the secondary symbiont *Wolbachia*, among
174 others (S2 Fig).

175

176 **2.2. CLas gene expression in the gut of adults of *Diaphorina citri***

177 Since we could not detect relevant read countings against transcripts belonging
178 to *Ca. L. asiaticus* when using samples obtained from nymphs, only samples collected
179 at the adult stage were subjected to differential expression analysis. Gene
180 expression analysis recognized 807 transcripts belonging to *Ca. L. asiaticus* in the gut of
181 adult psyllids fed on CLas-infected citrus plants in at least one of feeding exposure
182 periods analyzed for adults (1-2 d; 3-4 d; 5-6 d), with no CLas-related transcripts being
183 identified in gut samples from insects fed on healthy plants (*CLas*⁻).

184 The detection of gene expression of *Ca. L. asiaticus* in adult psyllids increased in
185 adults feeding on CLas-infected plants for 1-2 d to 5-6 d. Thus, 725 transcripts of CLas
186 were expressed in *A1CLas*⁺, 766 in *A2CLas*⁺ and 804 in *A3CLas*⁺ (Fig 1). One
187 transcript was expressed only in *A1CLas*⁺ and *A2CLas*⁺, 22 in *A1CLas*⁺ and *A3CLas*⁺,
188 and 63 in *A2CLas*⁺ and *A3CLas*⁺. We also identified CLas genes that were exclusively
189 expressed at the early (1-2 d, *A1CLas*⁺= 1 transcript, DN14421_c0_g2_i2 = nicotinate-
190 nucleotide adenylyltransferase), intermediate (3-4 d, *A2CLas*⁺= 1 transcript,
191 DN18703_c1_g1_i24 = Flp type IVb pilin) and late stage (5-6 d, *A3CLas*⁺= 18
192 transcripts) after adult started feeding on CLas-infected citrus plants (Fig 1). Most of
193 these transcripts were represented by several isoforms of a gene, with different isoforms
194 expressed in more than one of the sampled feeding times. Only *A3CLas*⁺ adults had
195 transcripts represented by unique isoforms of a gene specifically expressed in their gut
196 (Table 1).

197 **Table 1.** Single isoforms of *Candidatus Liberibacter asiaticus* transcripts exclusively
198 expressed in the gut of adult psyllids after 5-6d of feeding (*A3CLas*⁺) on CLas-infected
199 citrus plants.

200

Transcript ID	Annotation	TPM count
---------------	------------	-----------

DN1443_c0_g1_i1	hypothetical protein PSGCA5_05	58.77
DN15414_c0_g1_i2	pyridoxine 5'-phosphate synthase	5.33
DN25987_c0_g1_i1	hypothetical protein	30.77
DN32802_c0_g1_i1	anti-repressor protein	38.31
DN39169_c0_g1_i1	hypothetical protein BWK56_05555	69.16
DN44737_c0_g1_i1	threonine-tRNA ligase	168.28
DN47430_c0_g1_i1	flagellar basal body rod protein FlgF	54.15
DN55271_c0_g1_i1	phage related protein	10.66
DN62541_c0_g1_i1	flagellar basal body P-ring protein FlgI	31.40
DN64078_c0_g1_i1	putative phage-related acetyltransferase	43.56

201

202 Pairwise gene expression analysis of CLas in the gut of adult psyllids after
203 different periods of feeding on CLas-infected citrus plants revealed a high number of
204 differentially expressed CLas genes in *A3CLas⁺* as compared to *A1CLas⁺* and *A2CLas⁺*
205 adults (S1 Table). One-hundred transcripts out of the over 700 transcripts detected in
206 the three sampling times differed in their abundance (S1 Table). Differences in the level
207 of expression were detected for 80 transcripts when comparing *A1CLas⁺* and *A3CLas⁺*
208 and 20 transcripts in comparisons of *A2CLas⁺* and *A3CLas⁺* (S1 Table). CLas
209 expression was always higher in *A3CLas⁺* when compared to the others. No differences
210 in gene expression between *A1CLas⁺* and *A2CLas⁺* were detected (S1 Table).

211

212 **2.3. Differential gene expression in the gut of *CLas⁺* and *CLas⁻* adults of *Diaphorina***
213 *citri*

214 Differential gene expression (DE) of the gut of adults of *D. citri* after feeding on
215 CLas-infected plants for 1-2 days identified 24 DE transcripts in the gut of *CLas⁺*
216 insects, 20 of them were up-regulated and 4 were down-regulated in response to CLas
217 infection. Most of the up-regulated transcripts (11) belong to uncharacterized proteins,
218 while nine up-regulated transcripts were identified (Table 2). After 3-4 days of feeding

219 on CLas-infected plants, the number of DE transcripts in the gut of *CLas*⁺ as compared
220 to *CLas*⁻ adult psyllids increased to 35, most of which were up-regulated (27). Eighteen
221 out of the 27 up-regulated transcripts, and seven out of the eight down-regulated
222 transcripts were putatively identified (Table 2). The number of DE transcripts in the gut
223 of adult psyllids after 5-6 days of feeding on CLas-infected plants was the highest, with
224 61 DE transcripts in the gut of *CLas*⁺ insects, 57 (33 unknown proteins) of them were
225 up-regulated and 4 were down-regulated when compared to *CLas*⁻ adult psyllids (Table
226 2).

227 **Table 2.** List of genes difference expressed comparison of *Diaphorina citri* adults fed
228 on *Candidatus Liberibacter asiaticus* infected and non-infected plants at different
229

Stage	DE	Annotation	Transcript ID	FC	FDR
*A1 - CLas ⁺ x CLas ⁻	Up-regulated	arylsulfatase B-like isoform X1	DN19237_c6_g3_i2	20.9	2.0e ⁻²
		CLIP domain-containing serine protease 2-like isoform X1	DN16851_c1_g2_i2	119.9	3.0e ⁻³
		kinesin-like protein KIF3B isoform X4	DN10161_c0_g1_i1	55.2	6.1e ⁻³
		membrane metallo-endopeptidase-like 1 isoform X2	DN16798_c0_g1_i1	49.0	4.8e ⁻⁴
		methylglutaconyl-CoA hydratase, mitochondrial	DN18628_c4_g1_i2	26.7	1.0e ⁻²
		mitochondrial cytochrome c oxidase subunit IV	DN18774_c0_g1_i7	44.2	2.3e ⁻⁶
		nuclear speckle splicing regulatory protein 1-like	DN17904_c2_g1_i3	133.9	4.0e ⁻²
		uncharacterized protein LOC103515486	DN16253_c6_g2_i4	11.3	9.64e ⁻³
		protein phosphatase 1 regulatory subunit 21	DN19112_c0_g1_i1	36.7	0.02
		putative rna-directed dna polymerase from transposon bs	DN20114_c0_g1_i11	26.6	0.05
		uncharacterized protein LOC103508016	DN17144_c6_g5_i2	83.6	2.93e ⁻⁵
		uncharacterized protein LOC103508016	DN17144_c6_g5_i3	62.7	0.02
		uncharacterized protein LOC103518490	DN15191_c0_g1_i1	222.8	2.03e ⁻³
		uncharacterized protein LOC103518490	DN15191_c0_g1_i4	41.0	6.75e ⁻³
		uncharacterized protein LOC103519237	DN15191_c0_g1_i7	210.2	1.06e ⁻⁴
		uncharacterized protein LOC113469268	DN20635_c0_g3_i1	242.2	1.06e ⁻⁴
		uncharacterized protein LOC113469268	DN20635_c0_g1_i3	106.3	5.87e ⁻⁴
		uncharacterized protein LOC113471433	DN20585_c3_g1_i12	167.6	5.28e ⁻³
		uncharacterized protein PFB0145c-like	DN15546_c0_g1_i1	31.3	0.04

		uncharacterized protein YMR317W-like	DN15237_c0_g1_i1	132.6	4.69e ⁻⁴
Down-regulated	NADH dehydrogenase [ubiquinone] 1 beta subcomplex subunit 3	DN17549_c4_g1_i2	-32.5	6.75e ⁻³	
	protein pangolin, isoforms A/H/I/S-like	DN15424_c0_g3_i2	-28.0	0.03	
	titin isoform X7	DN21409_c5_g2_i1	-36.1	0.03	
	zonadhesin-like	DN14644_c0_g1_i1	-13.0	0.03	
Up-regulated	Ac1147-like protein	DN18394_c1_g1_i3	19.7	0.02	
	arylalkylamine N-acetyltransferase	DN20634_c1_g1_i13	45.9	0.05	
	cathepsin L1-like	DN15698_c4_g11_i2	111.4	1.45e ⁻³	
	hypothetical protein DAPPUDRAFT_37179, partial	DN18534_c0_g5_i1	17.0	7.51e ⁻⁴	
	hypothetical protein g.47064	DN18473_c2_g1_i1	11.7	8.68e ⁻³	
	hypothetical protein g.7198	DN16128_c4_g1_i1	11.1	3.86e ⁻³	
	large neutral amino acids transporter small subunit 1	DN20157_c2_g3_i2	66.6	1.50e ⁻⁴	
	nocturnin isoform X1	DN15927_c10_g1_i6	15.1	2.82e ⁻⁴	
	predicted protein	DN21032_c17_g1_i2	27.0	2.19e ⁻³	
	predicted protein	DN21032_c17_g1_i1	23.9	6.41e ⁻³	
	uncharacterized protein LOC105736982	DN21288_c9_g7_i2	28.5	8.64e ⁻⁴	
	uncharacterized protein LOC103515486	DN16253_c6_g2_i4	12.6	0.04	
	profilin	DN19422_c2_g2_i1	162.4	7.00e ⁻⁹	
	protein hu-li tai shao	DN19744_c0_g2_i2	12.2	0.01	
	putative senescence-associated protein	DN18133_c2_g1_i3	28.0	1.41e ⁻³	
	Regulator of rDNA transcription protein 15	DN16244_c2_g3_i1	24.8	1.62e ⁻³	
	Regulator of rDNA transcription protein 15	DN21288_c9_g7_i1	16.4	6.43e ⁻³	
	Regulator of rDNA transcription protein 15	DN16244_c2_g3_i2	15.6	7.58e ⁻⁴	
	Regulator of rDNA transcription protein 15	DN16244_c2_g3_i3	13.0	5.46e ⁻³	
	reverse transcriptase-like protein	DN21162_c2_g1_i4	12.4	0.02	
**A2 - CLas⁺ x CLas⁻	sodium/potassium-transporting ATPase subunit alpha-like	DN14485_c0_g1_i1	17.9	5.33e ⁻⁴	
	UNC93-like protein MFSD11	DN16539_c2_g6_i1	48.5	0.04	
	Uncharacterized protein ART2	DN19721_c0_g1_i3	9.8	0.02	
	uncharacterized protein LOC105206152	DN18133_c2_g1_i1	22.8	1.45e ⁻³	
	uncharacterized protein LOC105693632	DN19721_c0_g4_i1	7.9	8.56e ⁻³	

		uncharacterized protein LOC113219380	DN19326_c1_g1_i2	35.7	6.21e ⁻⁴
		uncharacterized protein LOC113469268	DN20635_c0_g1_i1	37.4	0.02
Down-regulated		leptin receptor overlapping transcript-like 1	DN20058_c2_g3_i4	-26.7	0.02
		methylglutaconyl-CoA hydratase, mitochondrial	DN18628_c4_g1_i2	-11.3	1.27e ⁻³
		putative juvenile hormone binding protein	DN21423_c1_g12_i2	-12.3	0.04
		Soluble NSF attachment protein	DN21196_c2_g1_i1	-19.8	5.64e ⁻⁷
		translation elongation factor 2	DN21188_c1_g7_i2	-11.9	0.02
		tubulin-folding cofactor B	DN17504_c3_g2_i6	-4.5	1.82e ⁻³
		uncharacterized protein LOC103513992	DN16335_c5_g1_i1	-16.7	5.18e ⁻³
		zinc transporter ZIP10 isoform X1	DN19132_c8_g1_i5	-43.4	0.02
Up-regulated		2-oxoglutarate dehydrogenase, mitochondrial-like	DN14833_c0_g1_i1	8.6	0.03
		Ac1147-like protein	DN21090_c8_g2_i1	50.3	0.04
		BCL2/adenovirus E1B 19 kDa protein-interacting protein 3	DN20168_c2_g3_i4	21.0	0.04
		beta-1,3-galactosyltransferase 5-like	DN18243_c2_g2_i2	20.2	7.31e ⁻³
		cleavage and polyadenylation specificity factor subunit CG7185-like	DN15201_c0_g1_i1	15.6	6.05e ⁻³
		cytochrome P450-like TBP	DN19721_c0_g1_i4	35.7	0.05
		dynein heavy chain 7, axonemal-like	DN35915_c0_g1_i1	17.3	0.05
		gamma-glutamyl hydrolase-like	DN18300_c5_g1_i2	16.7	3.96e ⁻⁵
		GATA zinc finger domain-containing protein 14-like	DN16387_c3_g2_i1	12.2	6.66e ⁻³
		glycerophosphocholine phosphodiesterase GPCPD1-like isoform X1	DN15741_c0_g2_i2	41.6	1.10e ⁻⁴
		hydrocephalus-inducing protein homolog	DN14616_c0_g1_i2	26.6	0.03
		hydrocephalus-inducing protein homolog	DN14616_c0_g2_i2	16.6	0.02
		hypothetical protein ALC57_18598	DN17391_c0_g1_i2	230.6	1.56e ⁻⁴
		hypothetical protein FF38_03795	DN18516_c0_g3_i1	67.0	0.02
		hypothetical protein LOTGIDRAFT_202939	DN17968_c0_g2_i3	101.2	0.03
		hypothetical protein Phum_PHUM590900	DN17430_c2_g2_i1	24.2	0.02
		keratin-associated protein 5-3-like	DN15230_c0_g1_i2	14.2	6.76e ⁻⁴
		keratinocyte proline-rich protein-like	DN20284_c2_g1_i3	11.5	0.02
		mucin-5AC-like, partial	DN16207_c6_g5_i1	7.7	0.04
		uncharacterized protein LOC103511862	DN17183_c5_g2_i3	9.4	0.04

***A3 - CLas⁺ x CLas

uncharacterized protein LOC103513455	DN17270_c3_g2_i1	46.8	0.04
uncharacterized protein LOC103514633	DN18467_c1_g5_i1	31.7	$3.61e^{-5}$
uncharacterized protein LOC103515486	DN16253_c6_g2_i4	12.6	0.04
uncharacterized protein LOC103518002	DN18156_c6_g2_i2	10.0	0.03
uncharacterized protein LOC103521603	DN17270_c3_g2_i2	63.7	0.01
uncharacterized protein LOC103521674	DN15182_c0_g1_i1	9.3	0.03
protein AMN1 homolog	DN15340_c0_g1_i1	8.9	0.04
protein FAM133-like isoform X1	DN19474_c1_g3_i11	15.4	$8.40e^{-3}$
protein PRRC2C-like	DN15390_c0_g1_i1	21.0	$3.47e^{-4}$
protein suppressor of forked	DN20501_c1_g1_i2	50.7	0.04
putative juvenile hormone binding protein	DN21423_c1_g12_i1	33.0	$5.4e^{-5}$
putative juvenile hormone binding protein	DN21423_c1_g12_i2	9.4	$8.34e^{-3}$
RNA-directed DNA polymerase from mobile element jockey-like	DN19725_c3_g1_i3	14.1	$6.95e^{-3}$
senescence-associated protein	DN16041_c1_g1_i2	198.7	$1.67e^{-4}$
SWI/SNF chromatin-remodeling complex subunit SNF5-like	DN18520_c6_g1_i1	52.5	$1.18e^{-5}$
uncharacterized protein Dyak_GE27401	DN16348_c2_g1_i1	18.0	0.02
uncharacterized protein LOC103507494 isoform X2	DN20548_c5_g2_i7	13.1	0.01
uncharacterized protein LOC103507496	DN20260_c2_g2_i2	17.0	$6.6e^{-4}$
uncharacterized protein LOC103507787	DN20585_c3_g1_i2	60.0	$8.58e^{-3}$
uncharacterized protein LOC103512709	DN20458_c5_g2_i2	29.7	0.03
uncharacterized protein LOC103514651	DN18692_c1_g1_i7	41.1	$9.13e^{-4}$
uncharacterized protein LOC103516995	DN14754_c0_g3_i1	39.3	$2.89e^{-3}$
uncharacterized protein LOC103518490	DN15191_c0_g1_i2	105.3	0.05
uncharacterized protein LOC103518490	DN15191_c0_g1_i4	85.7	$7.47e^{-3}$
uncharacterized protein LOC103519237	DN15191_c0_g1_i7	36.9	0.01
uncharacterized protein LOC103520317	DN17514_c8_g2_i1	10.7	0.01
uncharacterized protein LOC103524424	DN14888_c0_g2_i1	7.8	0.04
uncharacterized protein LOC108252545 isoform X1	DN16387_c3_g1_i9	7.6	0.03
uncharacterized protein LOC113219351	DN17193_c2_g1_i6	74.5	$8.74e^{-4}$
uncharacterized protein LOC113219380	DN18715_c0_g1_i6	305.6	$9.53e^{-5}$
uncharacterized protein LOC113219380	DN21090_c7_g10_i1	82.0	0.04
uncharacterized protein LOC113469268	DN20635_c0_g3_i2	73.8	0.03
uncharacterized protein LOC113469268	DN20635_c0_g1_i1	37.4	0.02

uncharacterized protein LOC113469268	DN20635_c0_g3_i1	36.9	0.02	
uncharacterized protein LOC113469388	DN14497_c0_g1_i2	8.9	0.04	
uncharacterized protein YMR317W-like	DN15237_c0_g1_i1	60.2	8.52e ⁻⁴	
Zgc:165536 protein	DN19721_c0_g2_i1	186.9	8.52e ⁻⁴	
<hr/>				
Down-regulated	annexin B9-like isoform X1	DN19784_c8_g1_i2	-11.0	0.03
	cytosolic purine 5'-nucleotidase isoform X4	DN16811_c2_g1_i5	-37.4	0.02
	probable 4-coumarate--CoA ligase 1	DN19422_c2_g3_i12	-7.4	0.05
	UDP-glucuronosyltransferase 2C1-like	DN20095_c3_g1_i5	-12.4	1.92e ⁻³

230 * A1- *CLas*⁺ x *CLas*⁻: Differential gene expression of adults with 1 to 2 days of
231 feeding; ** A2- *CLas*⁺ x *CLas*⁻: Differential gene expression of adults with 3 to 4 days
232 of feeding; *** A3- *CLas*⁺ x *CLas*⁻: Differential gene expression of adults with 5 to 6
233 days of feeding
234

235 From the total number of differentially expressed transcripts of *CLas*⁺ when
236 compared to their respective *CLas*⁻ psyllids, only one transcript was differentially
237 expressed in *CLas*⁺ psyllids regardless the time they were allowed to feed on *CLas*⁻
238 infected citrus plants as compared to psyllids fed on *CLas*-uninfected citrus plants (Fig
239 2). Most of the DE transcripts detected in *CLas*⁺ psyllids differed only at the specific
240 stage they were compared. Seventeen (71%) of the DE transcripts detected in the gut of
241 adult psyllids after 1-2 d, 31 (88%) after 3-4 d and 60 (88%) after 5-6 d of feeding in
242 *CLas*-infected plants differed from controls specifically at each particular stage (Fig 2).
243

244 3. Discussion

245 The gut differential gene expression in adult psyllids differed depending on the
246 duration of feeding on *CLas*-infected citrus plants. Longer was the duration of feeding
247 on *CLas*-infected citrus plants, higher were the number of DE transcripts. Most
248 interesting, the majority of DE transcripts detected were specific to each one of the
249 periods of feeding psyllids remained exposed to *CLas*-infected plants.

250 Gene expression of CLas in the gut of adult psyllids after different times of
251 feeding on CLas-infected citrus plants were quite different. CLas transcription in the gut
252 of adult psyllids was highly active soon after adult feeding started, but expression of a
253 large set of genes was significantly increased at later stages of feeding (*A3CLas*⁺).

254

255 **Immune attack and immune defense responses**

256 Bacteria that gain access to the hemocoel of insects find an easy way through the
257 gut epithelium of the midgut, once the epithelium in this region does not have the
258 cuticle lining protecting the fore- and the hindgut. Psyllids, as other sap-feeding insects
259 do not carry the peritrophic membrane that protects the midgut epithelium of several
260 other groups of insects (Lehane & Billingsley 1996, Erlandson et al. 2019). But
261 regardless the presence of such physical barriers, the front line of defense of the gut
262 immune system involves the activation of the epithelial innate immune system for the
263 production of reactive oxygen species (ROS). Bacteria that survive in the gut of insects
264 are either resistant to or are able to metabolize ROS (Buchon et al. 2013, Vallet-Gely et
265 al. 2008).

266 Analysis of the CLas gene expression in the gut of adult psyllids demonstrated
267 that CLas expressed the cytoprotective antioxidant enzyme peroxiredoxin
268 (DN17546_c4_g1_i1), capable of reducing ROS and reactive nitrogen species (RNS)
269 produced in the process of gut infection (Perkins et al., 2015; Knoops et al., 2016). The
270 significant increase in the expression of peroxiredoxin from *A1CLas*⁺ to *A3CLas*⁺ (FC =
271 13.48) indicates this enzyme provides an increased contribution in the infection process
272 as CLas cells also established an intracellular interaction with the gut epithelium of
273 psyllids. CLas expression of peroxiredoxin occurred despite the expected reduction of
274 ROS in the gut epithelium of adult psyllids, as the major source for ROS production in

275 the gut, NADH dehydrogenase [ubiquinone] 1 beta subcomplex subunit 3
276 (DN17549_c4_g1_i2), was down-regulated in *CLas*⁺ psyllids.

277 These results suggest that CLas can inhibit hydrogen peroxide production in the
278 host insect, and that peroxiredoxin is certainly serving roles other than its antioxidative
279 contribution. The adipokinetic hormone (ADK) is involved in the regulation of the
280 oxidative stress response in insects (Kodrik et al. 2015). Unfortunately, the expression
281 levels of ADK-related genes by CLas infection could not be verified as ADK is
282 produced and stored in neurosecretory cells of the *corpora cardiaca*. Nevertheless,
283 regulation of this neuropeptide hormone in the gut epithelium of *CLas*⁺ psyllids could
284 occur by the up-regulation of the metallo-endopeptidase-like 1 isoform X2
285 (DN16798_c0_g1_i1) neprilysin. Neprilysins are metalloproteases better known for
286 their neuropeptide degrading activity, while also carrying peptide-degrading activity in
287 other tissues, including the gut (Turner et al. 2001).

288 CLas peroxiredoxin could also be acting in the regulation of H₂O₂-mediated cell
289 signaling processes, such as those involved in growth and immune responses (Shears &
290 Hayakawa 2019). The oxidative response produced by gut epithelia due to microbial
291 infection leads to cell proliferation and modulation of the innate immune response
292 (Neish 2013), and ROS is required for inducing nitric oxide production in the gut. Nitric
293 oxide production will in turn trigger the synthesis of antimicrobial peptides (AMP) and
294 activate organ-to-organ communication (Wu et al. 2012). Therefore, the down-
295 regulation of ROS production in the gut of *CLas*⁺ psyllids could explain the lack of
296 differential expression of genes belonging to the AMP production pathways. AMP
297 synthesis can also be elicited by the recognition of peptidoglycans released by bacteria
298 by membrane-bound peptidoglycan recognition proteins if peptidoglycans survive to
299 amidase degradation (Vallet-Gely et al. 2008).

300 There is very little information on insect gut phagocytosis, although proteomic
301 analysis of anal droplets of the beetle *Cryptorhynchus lapathi* larvae led to the
302 identification of several proteins to support an immune cellular response at the gut level
303 (Jing et al. 2018). Moreover, phagocytic receptors identified in the gut epithelium of
304 *Drosophila* were proven to play crucial role in the phagocytosis of both Gram bacteria,
305 and in controlling hemocele infection by bacteria invasion through the gut epithelium
306 (Melcarne et al. 2019). We could not detect any changes at the molecular level in *CLas*⁺
307 psyllids that would demonstrate a phagocytic response in the gut, as well as we did not
308 observe adult psyllids to build an immune response to CLas infection by activating ROS
309 and AMP pathways.

310 Nevertheless, differential gene expression analysis of the gut of *A1CLas*⁺
311 psyllids demonstrated the mounting of a defensive response of the gut epithelium based
312 on the increased expression of a CLIP domain-containing serine protease 2-like
313 (DN16851_c1_g2_i2). CLIP domain-containing serine protease 2-like has been recently
314 reported to be up-regulated in the midgut of CLas-infected psyllids (Yu et al., 2020).
315 Serine proteases containing a CLIP domain are involved in the regulation of humoral
316 responses through the activation of prophenoloxidases (PPO) and the Toll immune
317 signaling pathway. Activation of Toll pathway leads to antimicrobial peptides
318 production, while the activation of PPO results in melanogenesis (Anderson 2000;
319 Nakhleh et al. 2017). Toll activation requires a multi-step proteolytic cascade (Stokes et
320 al. 2015), and the lack of additional differentially expressed serine proteases and the
321 antimicrobial peptides transcripts in the psyllid transcriptome support the argument that
322 the up-regulation of CLIP-domain serine protease in the gut of ACP feeding on CLas-
323 infected plants leads to the activation of melanization as an immune response against
324 CLas infection. We also believe the activation of melanization at this stage of psyllid-

325 CLas interaction was triggered by a local response caused by cell injury and invasion of
326 the gut epithelium by CLas cells, resulting in the production of wound clots in order to
327 avoid infected, damaged cells to suffer further damage, die and be replaced by *nidi*
328 cells. This hypothesis is also supported by the down-regulation of pangolin (*Pan*)
329 (DN15424_c0_g3_i2), a key regulator of the Wnt/Wg pathway. Wnt proteins are highly
330 conserved and participate in the control of growth, patterning, tissue and energy
331 homeostasis. Pangolin was reported to bind to the β -catenin homologue Armadillo,
332 acting directly in the regulation of gene expression in response to Wnt signaling
333 (Brunner et al. 1997; Franz et al. 2017). The Wnt signaling in *Drosophila* is an
334 important process for the homeostasis of the gut tissue as it is involved in the
335 regeneration of adult gut epithelial cells (Strand & Micchelli 2011, Cordero et al. 2012).
336 Thus, the down-regulation of pangolin interferes with the activation of the Wnt
337 signaling to regulate gene expression involved in the replacement of CLas-infected cells
338 by the activation of the *nidi* cells to differentiate into new, active cells of the gut
339 epithelium.

340 Studies on the role of genotype-genotype interactions of insects and parasites
341 demonstrated activation and differential gene expression of the host immune machinery
342 depending on the interacting parasite genotype. Alternative splicing was also reported as
343 a required element in the specificity of the immune response of insects to specific
344 parasite genotypes (Riddell et al. 2014). The nuclear speckles carry pre-mRNA splicing
345 machinery composed by nuclear speckle-related proteins that mediate alternative splice
346 site selection in targeted pre-mRNAs (Girard et al. 2012; Galganski et al., 2017). The
347 detected up-regulation of proteins that mediate alternative splice site selection in
348 targeted mRNAs, the nuclear speckle splicing regulatory protein 1-like

349 (DN17904_c2_g1_i3) in *CLas*⁺ psyllids, suggests CLas acts on the regulation of gene
350 expression of infected psyllids at the molecular level.

351 The psyllid initial defense response against CLas infection also included the up-
352 regulation of arylsulfatase B (DN19237_c6_g3_i2), an enzyme stored in lysosomes that
353 acts on large glycosaminoglycan molecules by removing attached sulfate groups
354 (Bhattacharyya et al., 2014). Glycosaminoglycans are components of proteoglycans
355 commonly exploited by pathogens as receptors for their adherence to different tissues
356 (García et al. 2016). Glycosaminoglycans are produced by some pathogenic bacteria as
357 extracellular capsule and used in the process of host infection and colonization to
358 facilitate pathogen attachment, invasion and/or evasion of host defensive mechanisms
359 (Roberts, 1996). Arylsulfatases B can also participate in processes of biotransformation,
360 mediating the sulfonation of xenobiotics by other enzymes to facilitate their excretion
361 (Zhao et al., 2016). In this case, increase in the arylsulfatase could be related to the
362 psyllid physiological needs to metabolize the high levels of flavonoids (hesperidin,
363 narirutin and dydimin) produced in citrus plants infected by *Ca. Liberibacter* (Massenti
364 et al., 2016; Dala-Paula et al., 2018; Kiefl et al., 2018). Flavanoids are important
365 metabolites produced by plants in response to abiotic and biotic stressors and play a
366 relevant contribution in plant resistance against microbes and herbivores (Treutter
367 2006), including citrus plants in response to CLas infection (Hijaz et al. 2013, 2020).

368 The overexpression of immune related genes and the required increased cell
369 metabolism early in the process of interaction of the psyllid gut epithelium with CLas
370 can explain the up-regulation of the mitochondrial cytochrome c oxidase subunit IV
371 (DN18774_c0_g1_i7) in *CLas*⁺ insects. Mitochondrial cytochrome c oxidase subunit IV
372 is the major regulation site for oxidative phosphorylation by catalyzing the final step of
373 electron transfer in mitochondria (Li et al. 2006b).

374

375 **Cross-talk in the colonization of the gut lumen**

376 Bacteria that survive the harsh chemical environment and the immune barriers
377 available in the gut will have to use strategies to avoid their rapid elimination from the
378 gut with faeces (Vallet-Gely et al. 2008, Benguettat et al. 2018). Insects are active
379 feeders and food fastly transits through the gut. The fast food transit in the gut has been
380 argued as one condition to explain the controversial lack of a resident microbiome in
381 lepidopteran larvae, for example (Hammer et al. 2017).

382 CLas seems to employ different strategies to colonize the gut lumen by avoiding
383 its elimination with faeces: regulation of gut peristalsis, synthesis of adherence proteins,
384 and biofilm formation.

385 CLas regulation of the psyllid gut peristalsis is thought to occur through the up-
386 regulation of the host neprilysin as earlier discussed. Neprilysins are reported to degrade
387 peptide hormones, and the gut of insects contains several hormone-producing cells.
388 Peptide hormones produced in the gut act as signaling molecules that are involved in the
389 regulation of a range of processes, including gut peristalsis (Wegener & Veenstra 2015,
390 Caccia et al. 2019, Wu et al. 2020). The hypothesis that CLas modulates the gut
391 peristalsis of psyllids is supported by the down-regulation of titin (DN21409_c5_g2_i1)
392 transcription in *CLas*⁺ psyllids. Muscle degeneration is marked by a reduction in titin
393 proteins, and gut-associated muscles are in charge of producing the peristaltic
394 movement observed in the gut. Additionaly, the intracellular non-catalytic domain of
395 neprilysins in excess is shown to induce muscle degeneration (Panz et al. 2012). Thus,
396 the degeneration of muscles associated with the gut would certainly impair gut
397 peristalsis and consequently reduce the elimination of bacteria with faeces (Vallet-Gely
398 et al. 2008, Benguettat et al. 2018).

399 Regulation of signaling in the gut is also evidenced by the up-regulation of
400 arylalkylamine N-acetyltransferase (DN20634_c1_g1_i13) transcription in *A2CLas*⁺
401 psyllids. Arylalkylamine N-acetyltransferases are involved in the N-acetylation of
402 arylalkylamines, playing an important role in the synthesis of melatonin in vertebrates
403 and invertebrates (Klein 2007; Hiragaki et al. 2015). But in insects, arylalkylamine N-
404 acetyltransferases also inactivate arylalkamines that play important roles as
405 neuromodulators, such as octopamine, dopamine and serotonin (Brodbeck et al. 1998;
406 Amherd et al. 2000). These neuromodulators are also implicated in the double brain-gut
407 communication circuitry (Solari et al. 2017; Zhang et al. 2018).

408 CLas adherence to the psyllid gut was achieved by the expression of three genes
409 of a subtype of the type IVb pilins, the tight adherence pili (Tad = Flp). Flp pilins are
410 common to several Gram⁺ and Gram⁻ bacteria. Type IV pili are highly diverse and
411 involved in a number of protein-protein interactions, but flp pili are better known for
412 their role in adherence to living and nonliving surfaces. Pili are also involved in cell
413 motility, secretion of exoproteins, and in host cell manipulation under extreme
414 conditions (Giltner et al. 2012, Kazmierczak et al. 2015).

415 The expression of Type IVc pili of *Ca. L. asiaticus* was reported to be higher in
416 psyllids than in plants, but only one (*flp3 pilin*) out of five *flp* genes was reported to be
417 up-regulated in psyllids (Andrade & Wang 2019). The *flp3 pilin* gene was demonstrated
418 to be under the regulation of VisN and VisR, demonstrating these proteins are important
419 in the colonization of the host vector (Andrade & Wang 2019). In our analysis of the
420 transcriptional profile of CLas in the gut of adult psyllids, we detected the expression of
421 several isoforms of two *flp* genes (DN14425_c0_g1; DN18703_c0_g1), but both
422 belonging to the family Type IVb pilin. Three isoforms of gene DN14425_c0_g1
423 (DN14425_c0_g1_i2; DN14425_c0_g1_i3; DN14425_c0_g1_i4) and two of gene

424 DN18703_c0_g1 (DN18703_c0_g1_i21 and DN18703_c0_g1_i23) were highly and
425 consistently expressed in the gut of psyllids in all sampling periods. Three LuxR family
426 transcriptional regulators (DN1177_c0_g1_i1, DN14940_c0_g2_i1, and
427 DN38633_c0_g1_i1) were also observed in the gut of *CLas*⁺ psyllids; nevertheless,
428 none of them was identified as the VisR or VisN regulators of *flp3 pilin* gene reported
429 by Andrade & Wang (2019).

430 The expression of CLas flagellins (*FlgA*) (DN3624_c0_g2_i1 and
431 DN40834_c0_g1_i1) and several genes involved in the assembling and functioning of
432 the flagellar machinery (*FliE*, *FliF*, *FliG*, *FliK*, *FliN*, *FliR*, *FliP*, *FlgB*, *FlgD*, *FlgE*,
433 *FlgF*, *FlgG*, *FlgH*, *FlgI*, *FlgK*, *FlhA*, *FlhB*, *MotB*, and the *flagellar C-ring protein*)
434 would indicate CLas assembles flagella for colonizing the gut of adult psyllids, although
435 *FlgF* and *FlgI* were detected exclusively in *A3CLas*⁺. The expression of genes involved
436 in the flagellar machinery corroborates recent data on the higher expression of genes
437 encoding the flagellum apparatus of CLas in the gut of psyllids than in plants (Andrade
438 et al. 2020a). Although we detected a much higher number of transcripts of the flagellar
439 system of the CLas isolate we worked with than those reported to be expressed in the
440 gut of psyllids by Andrade et al. (2020a), we did not detect the expression of three
441 genes they evaluated (*fliQ*, *fliL*, and *flgA*). Differences in the overall number of genes of
442 the flagellar system among lineages are expected to occur, but not among isolates of the
443 same species (Bardy et al. 2003).

444 The production of flagellum in the gut by infecting CLas is also supported by
445 transmission electron microscopy images, although most of the CLas cells observed
446 lacked a flagellum (Andrade et al. 2020a). Analysis of images of the flagellum of CLas
447 cells clearly shows CLas carries the secondary flagellar system, producing a lateral
448 flagellum. The secondary flagellar systems arose twice in the evolution of bacteria, once

449 in alpha-proteobacteria and once in the common ancestor of beta/gamma-proteobacteria
450 (Liu & Ochman 2007). The primary flagellar system produces a polar flagellum and
451 contributes with cell motility in liquid media, while the secondary flagellum system
452 produces a lateral flagellum that is involved in adhesion and cell swarming on surfaces.
453 Bacterial flagella serve bacteria not only as a motor apparatus, but also as a protein
454 export/assembly apparatus. The motor apparatus of flagella can provide bacteria the
455 movement required to remain in the gut, as demonstrated in the trypanosomatid
456 *Vickermania* (Kostygov et al. 2020). Moreover, the flagellum pattern can be altered by
457 bacteria depending on the environmental conditions faced, and bacterial flagella are
458 recognized as important virulence factors (Moens & Vanderleyden 1996, Macnab 2003,
459 Duan et al. 2013). Chemotaxis is an important contribution of bacterial flagellum to
460 virulence (Matilla & Krell 2018), and the detection of the expression of four chemotaxis
461 protein genes (DN15199, DN31800, DN46197 and DN50630) suggests the flagellum
462 participates in cell adhesion to and swarming on the psyllid gut epithelium. Yet, we also
463 propose the flagellum aids CLas to become chemically oriented for the localization of
464 suitable host cells for invasion.

465 Biofilm formation requires bacteria to synthesize an extracellular matrix.
466 Biofilms include extracellular proteins, cell surface adhesins and subunits of flagella
467 and pili proteins (Fong & Yildiz 2015). We did not identify the expression of adhesins
468 in the transcriptome of CLas in the gut of adult psyllids. Nevertheless, several
469 chaperones were highly expressed, and many chaperones can act as adhesins in bacteria.
470 Additionally, we believe the cold shock protein (DN10086_c0_g2_i1) of CLas is also
471 playing key roles in biofilm formation. Cold shock proteins were demonstrated not only
472 to participate in biofilm formation but also to support cell adhesion and motility, and to

473 stimulate cell aggregation, interfering thus with virulence (Eshwar et al. 2017, Ray et al.
474 2020).

475

476 **Cross-talk for infecting the gut epithelium**

477 Several gut-associated bacterial symbionts of hemipterans enter in close contact
478 with epithelial cells to establish an intracellular phase through endocytosis (Nardi et al.
479 2019). CLas also enters the gut epithelium of psyllids through endocytosis, remaining
480 inside vacuoles formed from or surrounded by endoplasmic reticulum membrane
481 (Ghanim et al. 2017). The differential gene expression analysis of the gut of *CLas*⁺
482 psyllids led to the identification of transcripts involved with ultrastructural alterations of
483 the gut epithelial cells, allowing the identification of the molecular intermediates that
484 participate in the route CLas follows to invade the gut epithelium.

485 In addition to the regulation of the immune related responses earlier described in
486 the gut epithelium of *CLas*⁺ psyllids, epithelial cells of the gut were altered early in the
487 infection process (*A1CLas*⁺ adults). Alterations are perceived by the transcriptional
488 down-regulation of zonadhesin-like (DN14644_c0_g1_i1), a transcriptional response
489 already reported by Ramsey et al. (2015). Zonadhesin-like proteins represent an
490 expansion of the zonadhesin multi-domain proteins that are implicated in the binding of
491 sperm and egg in a species-specific manner. In the gut, zonadhesin-like proteins are
492 thought to function as mucins, and two zonadhesin-like proteins of *D. citri* were
493 previously predicted to be part of the extracellular matrix and to have a role in cell-cell
494 adhesion. Mucins protect the gut epithelium from microbial infections and inflammation
495 (Hansson 2012). Mucins are components of the perimicrovillar layer that in psyllids and
496 other paraneopterans (Silva et al. 2004) replaces the chitin-based matrix (peritrophic

497 membrane) that provides a protective barrier to the gut epithelial cells from pathogenic
498 bacteria (Kuraishi et al. 2011).

499 In vertebrates the mucin composition of the mucous layer can vary among gut
500 regions, with diet composition and gut microbial infection (Paone & Cani 2020).
501 Mucins can also be exploited as a nutritional resource by bacteria, and degradation of
502 mucins by a commensal microbe was demonstrated to facilitate the penetration of the
503 epithelium by viruses (Schroeder 2019, Wu et al. 2019). The role different mucins can
504 have on the host-pathogen interaction can explain the up-regulation of the psyllid gene
505 coding for mucin-5AC (DN16207_c6_g5_i1) in *A3CLas⁺* psyllids. The higher
506 abundance of this protein in *CLas⁺* psyllids has been demonstrated in previous
507 proteomic analysis (Ramsey et al. 2017). Regulation of the host mucin-5AC has been
508 reported in vertebrate hosts infected by Gram⁻ and Gram⁺ bacteria, and in one system
509 modulation of mucin-5AC has been linked with increased adhesion of bacteria to the
510 gut tissue (Dohrman et al. 1998, Quintana-Hayashi et al. 2015).

511 The differential expression of genes coding for cytoskeletal proteins involved in
512 the regulation of the submembranous actin-spectrin network in cells of the gut
513 epithelium of *CLas⁺* psyllids demonstrates CLas interferes with the remodeling of gut
514 epithelial junctions in adult psyllids, leading to endocytosis of intercellular junctions
515 with cellular organelles. Adducins (protein Hu-li tai shao - DN19744_c0_g2_i2) form
516 connections with membranes, promote spectrin-actin interactions and regulate actin
517 filaments (Matsuoka et al. 2000). Internalization of apical junction and/or tight junction
518 proteins may disrupt the epithelial barriers and favor the movement of bacterial toxins
519 into cells (Hopkins et al. 2003).

520 The intracellular events in preparation for endocytosis can also be detected as
521 indicated by the up-regulation of the psyllid phosphatase 1 regulatory subunit 21

522 (DN19112_c0_g1_i1) in the gut of *A1CLas*⁺. This protein participates in early (sorting
523 process) or late (maturation) endosome pathway, which leads to the endocytosis of
524 several types of materials, including pathogenic agents. Our hypothesis is that early
525 endosomes will also internalize the leptin receptor overlapping protein-like 1. The leptin
526 receptor overlapping transcript-like 1 (DN20058_c2_g3_i4) was down-regulated in the
527 gut epithelium of *A2CLas*⁺ psyllids. Internalization of such receptors in early
528 endosomes also affects cell signaling, and in this particular case can severely interferes
529 with the gut epithelium resistance to microbial infection. Down-regulation of
530 leptin/leptin receptor was reported to drastically affect cell resistance to amoeba and
531 bacterial infection in several species (Faggioni et al. 2001, Guo et al. 2011, Mackey-
532 Lawrence & Petri Jr 2012).

533 The endocytic vesicles detach and become free endocytic carrier vesicles
534 transporting their cargoes to late endosomes to finally fuse with endoplasmic reticulum,
535 where CLas cells aggregate in associated vacuoles as indicated by ultrastructural
536 analysis (Ghanim et al. 2017). Fusion of lysosomes to cell aggregates vacuoles is
537 inhibited by the down-regulation of soluble NSF attachment protein (SNAPs)
538 (DN21196_c2_g1_i1) in *A2CLas*⁺. SNAPs are highly conserved proteins that
539 participate in intracellular membrane fusion and vesicular trafficking (Stenbeck, 1998).
540 Intracellular membrane fusion requires both SNAPs and NSF to act in concert, and
541 inhibition of one of them will lead to the failure of membrane fusion and the
542 accumulation of vesicles one cannot fuse (Rothman, 1994).

543 SNAPs are characterized by the presence of a tetratricopeptide repeat (TPR)
544 domain (Lakhssassi et al., 2017). Tetratricopeptide repeat proteins (TRP) are directly
545 involved in virulence, particularly due the translocation of virulence factors into host
546 cells and in the blockage of phagolysosomal maturation, among others (Cerveny et al.

547 2013). Three TRPs (DN11192_c0_g1_i1; DN11192_c0_g1_i2; DN14826_c0_g1_i2)
548 were expressed in the gut of *CLas*⁺ psyllids, but only DN14826_c0_g1_i2 was
549 differentially expressed. The expression of different TRPs in all sampling periods and
550 their time-specific differential expression indicates TRPs participates in different
551 processes of CLas interactions with the host cells, from CLas establishment in the gut
552 lumen to epithelial cell invasion and access to the hemocoel.

553 The down-regulation of the psyllids annexin B9-like isoform X1
554 (DN19784_c8_g1_i2) in the gut of *A3CLas*⁺ would interferes with the development of
555 multivesicular bodies, once annexin B9 is involved in endosomal trafficking to
556 multivesicular bodies (Tjota et al. 2011). This change will affect the transfer of the
557 contents of CLas-containing endosomal vesicles to lysosomes for proteolytic
558 degradation.

559 We propose that the establishment of the intracellular cycle and survival of CLas
560 within host cells was putatively aided by the expression of CLas peptidyl-prolyl
561 isomerase (PPI) (DN14386_c0_g1_i1), a protein that has been proved to participate in
562 intracellular infection and virulence of other Gram⁻ bacteria (Norville et al. 2011,
563 Pandey et al. 2017, Rasch et al. 2018). The Mpi PPI from *Legionella pneumophila* was
564 demonstrated to require an active enzymatic site to enhance a proper host cell invasion
565 (Helbig et al. 2003), although the preservation of the active site was not a requirement
566 for the PPI of *Burkholderia pseudomallei* (Norville et al. 2011). Ghanim et al. (2017)
567 suggested earlier that CLas cells do not enter the ER, but instead CLas cells recruit ER
568 to transform the phagosome into a host-immune free space suitable for CLas survival
569 and multiplication. These same ER-derived structures were already observed in
570 *Legionella* and *Brucella* (Celli & Gorvel 2004, Robinson & Roy 2006).

571 Early endosomes and endoplasmic reticulum share contact sites that are used to
572 bind to microtubules at or close to their contact sites, and both organelles remain
573 bounded as endosomes traffic and mature (Friedman et al. 2013). Endosome trafficking
574 within the cell involves the membrane binding to motor proteins and its transport along
575 the actin and microtubule cytoskeleton (Granger et al. 2014). Trafficking of endosomes
576 in *CLas*⁺ psyllids is provided by the up-regulation of kinesin-like protein KIF3B
577 isoform X4 (DN10161_c0_g1_i1) in the gut of psyllids. Kinesins are motor proteins
578 involved in the movement of multiple cytoplasmic organelles (Granger et al. 2014).

579 Profilin (DN19422_c2_g2_i1), another protein involved in intracellular
580 movement of organelles, was also up-regulated in the gut of *A2CLas*⁺ psyllids. Profilins
581 are actin-binding proteins capable of regulating actin polymerization and the availability
582 of the actin cytoskeleton for binding to the endosomes; but new roles for profilins are
583 being identified in vertebrates (Witke 2004). Additionally, profilin 1 play an important
584 role in host-pathogen interactions. Intracellular pathogens such as *Listeria*
585 *monocytogenes* and *Shigella flexneri* use the host-cell actin cytoskeleton to propel
586 themselves through the cytoplasm and to spread to neighboring cells without entering
587 the extracellular space (Kocks, 1994; Witke, 2004). Dynein (DN35915_c0_g1_i1),
588 another motor protein, was up-regulated in the gut of *A3CLas*⁺ psyllids. Dyneins also
589 contribute to microtubule-based transport in eukaryotic cells (reviewed in Holzbaur &
590 Vallee, 1994; Porter, 1996; Hirokawa, 1998).

591

592 **Cross-talk for moving to the hemocoel**

593 After CLas inhibits the early immune response and invades the intracellular
594 space of the gut epithelium by regulating a clathrin-independent endocytosis
595 mechanism, hiding from the host's immune activators within vacuoles surrounded by

596 endoplasmic reticulum membrane, where CLas multiplies, the molecular mechanism
597 behind the release of CLas bacteria from epithelial cells in the hemocoel may require
598 additional data.

599 The higher expression in *AD3CLas⁺* of seven (DN15630_c0_g2_i3 =
600 CLIBASIA_00255; DN15330_c0_g1_i2 = CLIBASIA_00880; DN14809_c0_g1_i =
601 CLIBASIA_03170; DN14146_c0_g1_i1 = CLIBASIA_04410; DN10141_c0_g1_i1 =
602 CLIBASIA_00995; DN15141_c0_g1_i1 = CLIBASIA_01620; DN15414_c0_g1_i4 =
603 CLIBASIA_01605) out of the 67 Sec-dependent proteins common to Las species
604 (Thapa et al. 2020) indicates these candidate effector proteins play an important role in
605 the dynamics of CLas infection of the psyllid gut epithelium at this stage. In fact,
606 genomic analysis of *Liberibacter* species predicted a total of 166 proteins containing
607 Sec-dependent signal peptides in the CLas strain psy62, from which 86 have been
608 already experimentally validated (Prasad et al. 2016). These are potential effector
609 proteins, and 106 of them share common homologues with *Las_Ishi-1* and *Las_gxpsy*.
610 But only 45 Sec-dependent proteins were shared among HLB-associated *Ca.*
611 *Liberibacter* species (CLas, CLam and CLaf) (Wang et al. 2017; Andrade et al. 2020b).
612 The detection of transcripts of the general secretion system provides further support for
613 the participation of the detected Sec-dependent proteins in the late process of infection
614 of the gut epithelium of *D. citri*. The Sec pathway secretion system transports proteins
615 involved in bacterial cell functions and survival (Thapa et al. 2020). The Sec pathway is
616 represented by two independent pathways, both detected in the gut of *CLas⁺* psyllids:
617 the post-translational pathway represented by the expression of SecA
618 (DN14962_c0_g1_i1) and SecY (DN15568_c0_g3_i3); and the co-translational
619 pathway represented by the signal recognition particle receptor FtsY
620 (DN1686_c0_g1_i1) (Green & Mecsas 2016). We did not detect SecB expression in the

621 gut of adult psyllids, indicating SecA can also act as a chaperone complementing the
622 required activity of SecB as reported in *Escherichia coli* (McFarland et al. 1993).

623 Combined ultrastructure, proteomics and transcriptomics analysis of the gut
624 epithelium of CLas-infected psyllids suggested CLas acquisition into the hemocoel
625 would rely on the programmed cell death of CLas-infected epithelial gut cells, although
626 CLas infection has little impact on the fitness of adult psyllids (Kruse et al. 2017). The
627 low fitness impact of CLas infection to adult *D. citri* indicates CLas acquisition into the
628 hemocoel would occur through an exocytosis process, as suggested for the *Ca.*
629 *Liberibacter solanacearum* vectored by potato psyllids (Cicero et al. 2017).

630 By following the proposed subroutines based on mechanistic and essential
631 aspects of cell death proposed by the Nomenclature Committee on Cell Death (Galluzzi
632 et al 2018), our transcriptomic analysis could not support the proposition that CLas-
633 infected epithelial gut cells of psyllids would initiate the process of programmed cell
634 death (PCD) as proposed by Kruse et al. (2017). We did not observed transcription of
635 caspases, a very common protein to several subroutines of cell death, as well as other
636 aspects that would allow this characterization (Galluzzi et al 2018). Yet, we were unable
637 to confidently characterize one of the subroutines of cell death described when
638 analyzing the transcriptional profile of *CLas*⁺ psyllids, once the molecular mechanisms
639 involved were not all represented. However, we can confidently report the
640 activation/inhibition of the expression of genes involved in processes of regulated cell
641 death. The high expression of the lysosomal cathepsin L1 (DN15698_c4_g11_i2) in
642 *A2CLas*⁺ psyllids would support the activation of lysosome-dependent cell death, which
643 requires intracellular perturbations to permeabilize the lysosomal membrane to result in
644 the release of cytosolic cathepsins. Mitochondrial outer membrane permeabilization and
645 caspases are not necessarily required for this process of cell death, and lysosome-

646 dependent cell death is an important response to pathophysiological conditions induced
647 by intracellular pathogens (Galluzzi et al 2018).

648 The overexpression of the psyllid BCL2/adenovirus E1B 19 kDa protein-
649 interacting protein 3 (BNIP3) (DN_20168_c2_g3_i4) in *A3CLas⁺* also supports the gut
650 epithelium of *CLas⁺* psyllids go into lysosome-dependent cell death. BNIP3 are pro-
651 apoptotic proteins that open the pores of mitochondrial outer membrane, resulting in
652 mitochondria dysregulation due the loss of membrane potential and ROS production in
653 mitochondria (Vande Velde et al 2000, Moy & Cherry 2013). But BNIP3
654 oligomerization with BCL2 has been demonstrated not to be required for cell death
655 (Vande Velde et al. 2000). Besides, the down-regulation of the psyllid senescence-
656 associated protein transcript (DN16041_c1_g1_i2) in the gut of *A3CLas⁺* psyllids
657 demonstrates CLas suppresses cell senescence and the further dysfunctional growth of
658 the epithelial cells due the activation of senescence-associated secretory phenotype
659 (Münch et al 2008, Ito & Igaki 2016). Cellular senescence is not considered a form of
660 regulated cell death (Galluzzi et al 2018).

661 The differential expression of a putative juvenile hormone binding protein
662 (JHBP) (DN21423_c1_g12_i2; DN21423_c1_g12_i1) in *CLas⁺* psyllids (down-
663 regulation in the gut of *A2CLas⁺*; up-regulation in *A3CLas⁺*) demonstrates the epithelial
664 cells count with different levels of hormonal stimulation. JHBP are proteins that act as
665 shuttles for juvenile hormone (JH) in the hemolymph, avoiding JH degradation by JH-
666 esterases and JH-epoxide hydrolases (Zalewska et al., 2009). JH is produced and
667 released primarily by neurosecretory cells of the *corpora allata* of the central nervous
668 system, and the availability of JHBP in the gut, if its activity in the gut is the same
669 played in the hemolymph, indicates JH is also available in the gut epithelial cells. JH has
670 recently been shown to be produced by intestinal stem cells and enteroblasts of the gut

671 epithelium of *D. melanogaster*, and to regulate cell growth and survival. The local JH
672 activity was also shown relevant for damage response by gut cells, playing important
673 roles in gut homeostasis (Rahman et al 2017). If the pattern of expression of JHBP
674 correlates with the availability of JH we can argue that at the same time CLas acts on
675 the regulation of the gut epithelium by suppressing cell senescence, it can also induce
676 the proliferation of stem cells in order to replace cells that were damaged due the release
677 of CLas cell into the hemocoel and/or entered the lysosome-mediated cell death as
678 discussed earlier.

679 The observed up-regulation of the transcriptional levels of nocturnin
680 (DN19927_c10_g1_i6) in the gut of *A2CLas⁺* psyllids suggests that this circadian
681 rhythm effector protein may be acting together with JH in regulating gut genes, just as
682 the joint action of the circadian genes and JH in the regulation of genes acting on the
683 transitional states of *Pyrrhocoris apterus* adults to reproductive diapause or not (Bajgar
684 et al. 2013). Nocturnin is classified as a deadenylase acting on the catalysis of poly(A)
685 tail of target mRNAs and/or targeting noncoding RNAs, and has been implicated in
686 metabolic regulation, development and differentiation (Hughes et al. 2018). But recent
687 studies with *curled*, the nocturnin ortholog in *Drosophila* proved nocturnin is an
688 NADP(H)2'-phosphatase acting on the conversion of the dinucleotide NADP⁺ into
689 NAD⁺ and NADPH into NADH, regulating mitochondrial activity and cellular
690 metabolism in response to circadian clock (Estrella et al. 2019). NADP(H)2'-
691 phosphatase activity of nocturnin was later reported in vertebrates, with the
692 demonstration of the colocalization of nocturnin in mitochondria, cytosol and
693 endoplasmic reticulum-bound pools depending on the isoform (Laothamatas et al.
694 2020). Thus, nocturnin acts as a regulator of the intracellular levels of NADP(H) and
695 the oxidative stress response. The role of nocturnin in the regulation of cell metabolism

696 and the oxidative stress response supports the required energy supply to sustain the
697 increased gene expression activity in *CLas*⁺ gut epithelium cells.

698 The expression profile of CLas infecting the gut epithelium of *A3CLas*⁺ psyllids
699 demonstrates CLas has an increased protein synthesis activity as expected by the
700 overexpression of DEAD/DEAH box helicase (DN4052_c0_g1_i1), a protein involved
701 in ribosome biogenesis, RNA turnover and translation initiation (Redder et al., 2015).
702 Increased protein activity is also supported by the increased expression of molecular
703 chaperones, such as the trigger factor (DN13945_c0_g1_i1), GroEL
704 (DN14757_c0_g1_i1) and DnaK (DN15220_c0_g1_i1), which prevent protein
705 misfolding and aggregation (Agashe et al 2004, Merz et al. 2006).

706

707 **CLas multiprotein complexes**

708 The protein HlyD family efflux transporter periplasmic adaptor subunit
709 (DN11766_c0_g1_i1) and the outer membrane factor translocation protein TolB
710 (DN15087_c0_g1_i3) are essential components for functioning the pump of tripartite
711 efflux systems. HlyD connects primary and secondary inner membrane transporters to
712 the outer membrane factor TolB. CLas expressed several inner membrane transporters
713 belonging to the MSF and ABC families. TolB has been shown to interact with a range
714 of proteins including cell-killing proteins (Carr et al. 2000, Loftus et al. 2006). In
715 *Xylella fastidiosa* TolB was shown to be involved in biofilm development (Santos et al.
716 2015).

717

718 **Additional CLas transcriptional regulators**

719 The detection of several other uncharacterized response regulators
720 (DN10585_c0_g1_i1; DN10585_c0_g2_i1; DN12200_c0_g1_i1; DN58285_c0_g1_i1)

721 and transcriptional regulators (DN11066_c0_g1_i1; DN15145_c0_g1_i2;
722 DN15145_c0_g1_i5) indicates other CLas two-component systems are also being
723 activated by environmental stimuli, such as the two-component system sensor histidine
724 kinase AtoS (DN14305_c0_g2_i1; DN15701_c0_g1_i1). The two-component system
725 sensor histidine kinase AtoS is a member of the AtoS/AtoC regulatory system, but we
726 did not identify the AtoC response regulator in the CLas transcriptome. This regulatory
727 system is better known by the induction of AtoS by acetoacetate. AtoS then
728 phosphorylates AtoC that will in turn stimulate the expression of the *atoDAEB* operon
729 for the catabolism of short chain fatty acids. We could not reliably identify transcripts
730 belonging to the *atoDAEB* operon to demonstrate CLas requirements for short chain
731 fatty acids. We propose that the activation of the AtoS/AtoC regulatory system is
732 instead acting on the regulation of the flagellar regulon, regulating the expression of
733 CLas genes involved in cell motility and chemotaxis, as reported for *Escherichia coli* in
734 response to acetoacetate or spermidine (Theodorou et al. 2012).

735

736 **Cross-talk on nutrient deficiency**

737 The high expression of sulfonate ABC transporter permease
738 (DN15690_c0_g1_i2) in all *CLas*⁺ psyllids suggests CLas signals the host to supply its
739 requirements for sulfur. Sulfur is a ubiquitous element involved in a number of different
740 processes in organisms (Beinert 2000). The sulfonate ABC transporter permease is
741 involved in sulfur/sulfonate uptake, and the higher expression observed in *A3CLas*⁺ as
742 compared to *A1CLas*⁺ points for an increased demand late in the infection process.

743 Sulfur is also used in the biogenesis of Fe-S clusters, which are produced in
744 conditions of oxidative stress and iron deprivation. The biogenesis of Fe-S clusters was
745 observed by the expression of two unclassified cysteine sulfurases (DN12917_c0_g1_i1

746 and DN35541_c0_g1_i1), the cysteine desulfurization protein SufE (DN1144_c0_g1_i1),
747 the Fe-S cluster assembly protein SulfB (DN14252_c0_g1_i1), and the iron-sulfur
748 cluster carrier protein ApbC (DN17762_c4_g2_i3) (Layer et al. 2007, Roche et al.
749 2013). All four genes had an increased expression in *A3CLas*⁺ as compared to *A1CLas*⁺.
750 Sulfur requirements by CLas could also be used for protection against oxidative stress
751 as demonstrated by the expression of the thioredoxin-dependent thiol peroxidase
752 (DN10526_c0_g1_i1) (Lu & Holmgren 2014; Wang et al. 2020).

753 The high expression of CLas phosphate ABC transporter permease subunit PstC
754 (DN40256_c0_g1_i1; DN67283_c0_g1_i1), putative two-component sensor histidine
755 kinase transcriptional regulatory protein (DN14305_c0_g2_i1), two-component sensor
756 histidine kinase (PhoR) (DN28075_c0_g1_i1; DN67626_c0_g1_i1), two component
757 response regulator protein (PhoB) (DN14869_c0_g1_i1), alkaline phosphatase
758 (DN12828_c0_g1_i2; DN39297_c0_g1_i2) and NTP pyrophosphohydrolase
759 (DN2128_c0_g1_i1) demonstrates CLas cells are exposed to phosphate restriction while
760 infecting the gut epithelium of adult psyllids. Phosphate is generally the major source
761 of phosphorus to bacteria, a vital nutrient for living organisms. Phosphorus is important
762 in several processes (energy metabolism, intracellular signaling, among others).
763 Misregulation of phosphorus availability in bacteria is sensed by the PhoB/PhoR two-
764 component regulatory system, leading to the activation of the Pho regulon. The Pho
765 regulon regulates the expression of other genes, producing phenotypes that can differ in
766 morphology and virulence in response to phosphate deprivation (Lamarche et al. 2008,
767 Santos-Benito 2015). Thus, the expression of both members of the PhoB/PhoR two-
768 component regulatory system and the phosphate ABC transporter permease subunit
769 PstC, that is in charge to transport extracellular phosphate to the cytosol, proves CLas
770 was exposed to phosphate concentrations below 4 μ M, a threshold that generally turns

771 on the expression of the response regulator PhoB. Furthermore, the expression of
772 alkaline phosphatase and NTP pyrophosphohydrolase, which both act on phosphorus-
773 containing substrates (Lamarche et al. 2008) demonstrates CLas increased the
774 catabolism of substrates capable of releasing phosphorus nutrient.

775 The requirement of CLas for phosphate is also demonstrated by the up-
776 regulation of the psyllid glycerophosphocholine phosphodiesterase GPCPD1 gene, as
777 observed by the increased abundance of its transcript (DN15741_c0_g2_i2) in
778 *A3CLas*⁺. The contribution of GPCPD1 in phosphate production results from the
779 downstream processing of GPCPD1 hydrolysis products of glycerophosphocholine,
780 choline and glycerolphosphate. At the same time glycerophosphocholine hydrolysis can
781 provide phosphates for cell metabolism, the choline can serve as as substrate for
782 phosphatidylcholine synthesis. Phosphatidylcholine is a major lipid component of
783 membranes of eukaryotes, although several bacterial symbionts and pathogens carry
784 phosphatidylcholine synthases, showing their requirement for this lipid component of
785 cell membranes, including those belonging to *Rhizobiaceae* as *Ca. Liberibacter*. Choline
786 serves as substrate for the osmoprotectant glycine betaine synthesis and as an energy
787 substrate to support cell growth in *Rhizobiaceae* (Sohlenkamp et al., 2003; Dupont et
788 al., 2004).

789 The role of host-produced choline in CLas metabolism is supported by the up-
790 regulation of CLas glycine/betaine ABC transporter substrate-binding protein
791 (DN15178_c0_g1_i1) in the gut of *A3CLas*⁺. ABC transporters were reported to have
792 several important roles in *Ca. Liberibacter asiaticus*, from the importation of nutrients
793 like choline to the exportation of virulence factors (Li et al., 2012). Thus, we believe the
794 increased activity of GPCPD1 in *A3CLas*⁺ is a result of the recycling of
795 glycerophosphocholine for choline utilization in the recovery of membranes of the gut

796 epithelial cells of the host psyllid as a response to cell infection and/or in the
797 supplementation of choline to CLas metabolism.

798 CLas is known to induce profound physiological changes in citrus plants,
799 affecting the nutritional content of CLas-infected plants to psyllids, which have in turn
800 altered transcriptional profiles and protein abundance when feeding on CLas-infected
801 and healthy citrus plants (Fu et al. 2016, Ramsey et al. 2017). Therefore, it is impossible
802 to distinguish if the indication of nutritional restriction CLas encounters when infecting
803 the gut epithelium of psyllids is an indirect effect of the host plant on the psyllids or if
804 this is a direct response of psyllids to avoid CLas infection.

805

806 **4. Material and Methods**

807 **4.1. *Diaphorina citri* rearing and plants**

808 A colony of CLas-free Asian Citrus Psyllid (ACP) was initiated with insects
809 collected from *Murraya paniculata* (L.) Jack, syn. *Murraya exotica* L. (Sapindales:
810 Rutaceae) in the state of São Paulo, Brazil in 2009.

811

812 **4.2. *Diaphorina citri* gut collection and RNA extraction**

813 Adults of *D. citri* (7 to 10 days after emergence) were transferred to uninfected
814 and CLas-infected citrus plants [*Citrus x sinensis* (L.) Osbeck, grafted in ‘Rangpur’
815 lime (*C. x limonia* Osbeck)] for an exposure period (EP) of 1, 2, 3, 4, 5 and 6 days. For
816 each exposure period, three biological replicates were collected (1 replicate = 100
817 individuals). Third-instars of *D. citri* were also transferred to CLas-infected and
818 uninfected (control) citrus plants for collection of RNA and differential transcriptional
819 analysis. Nymphs were allowed to feed for 4 days on CLas-infected and control plants.

820 Afterwards, three biological replicates/treatment (1 replicate = 200 nymphs) were
821 collected and stored in RNALater for further processing and analysis.

822 After each exposure time, adults were collected and the gut dissected under
823 aseptic conditions. A similar procedure was used for nymphs, but in this case insects we
824 opted by extracting RNA from whole nymphs, as initial attempts to dissect the suitable
825 gut samples for downstream analysis were very time-consuming and had a low success
826 rate.

827 The obtained guts/nymphs were stored in RNALater (Invitrogen/ThermoFisher
828 Scientific, Waltham, MA, EUA) at -80°C until RNA extraction. Total RNA extraction was
829 performed using the SV RNA Isolation System Kit (Promega), following the
830 manufacturers' recommendations. Samples were lysed in 175 µL of RNA lysis buffer
831 added with β-mercaptoethanol and 350 µL of RNA dilution buffer for tissue disruption
832 using a TissueLyser II LT™ (Qiagen). Samples were incubated at 70°C for 3 min,
833 centrifuged (12,000 g × 10 min × 4°C), trapped in a column and washed with 95%
834 ethanol by centrifugation (12,000 g × 10 min × 4°C). Total RNA was recovered in 350
835 µL of RNA wash solution following centrifugation (12,000 g × 1 min × 4°C).
836 Afterwards, samples were treated with 50 µL of DNase mix (40 µL buffer 'yellow
837 core'+ 5 µL 0.09 M MnCl₂ + 5 µL DNase I) for 15 min at room temperature. Samples
838 were added with 200 µL of DNase stop solution and subjected to centrifugation
839 (13,000 g × 1 min × 4°C). Samples were washed in 600 µL cleaning solution followed
840 by a second wash in 250 µL following centrifugation (12,000 g × 1 min × 4°C). The
841 pelleted RNA was recovered in 30 µL of nuclease-free water, and RNA concentration
842 verified using NanoDrop V 3.8.1 (ThermoFischer).

843 RNA samples containing residual DNA contaminants were further treated with 2
844 µL of buffer (10×) and 2 µL of Turbo™ DNase (2 U/µL) (Ambion®). Samples were

845 incubated at 37°C for 30 min followed by DNase inactivation by adding 2 µL of
846 DNase Inactivation Reagent (Ambion®). After 5 min at room temperature, samples
847 were centrifuged (13,000 g × 1.5 min × 4°C) and the supernatant collected and stored at
848 -80°C. DNA elimination was confirmed by testing the amplification of the wingless
849 gene (*wg*) of ACP (Manjunath et al., 2008).

850 All plants and insects were subjected to quantitative PCR analysis for
851 verification of CLas infection using the TaqMan qPCR Master Mix Kit (Ambion®)
852 following Li et al. (2006a).

853 In insects, the average Ct value found for the *wg* gene in the libraries was 30.7,
854 while the average Ct value in plants for the 16S rRNA gene from CLas was 29.6.
855 Samples with a Ct value under 35 were considered positive for CLas.

856 After confirmation of the *Ca. L. asiaticus* infection status of each sample, RNA
857 obtained from the gut samples of adults were pooled in equimolar concentrations to
858 yield three exposure periods: *i) A1CLas-*: adults that fed on healthy citrus plant (CLas-)
859 for 1-2 days; *ii) A2CLas-*: for 3-4 days; *iii) A3CLas-*: for 5-6 days; *iv) A1CLas+*: adults
860 that fed on infected citrus plant (CLas+) for 1-2 days; *v) A2CLas+*: for 3-4 days; and *vi)*
861 *A3CLas+*: for 5-6 days. In the case of the whole nymphs, two samples were produced:
862 *N1CLas+*: for nymphs after 4 days of feeding on CLas-infected citrus plants, and
863 *N1CLas-*: for nymphs after 4 days of feeding on control plants.

864 Samples were subjected to mRNA enrichment through eukaryote and prokaryote
865 rRNA removal using the Ribo-Zero rRNA Removal Epidemiology Kit (Illumina®),
866 following the manufacturers' instructions. RNA integrity was confirmed using the
867 Agilent Bioanalyzer 1000 (Agilent Technologies).

868

869 **4.4. Library preparation and sequencing**

870 cDNA libraries were prepared for sequencing using the cDNA TruSeq RNA
871 Library Prep Kit (Illumina®) following a paired-end (2 × 100 bp) strategy. The cDNA
872 produced was end-repaired and adenosine was added at the 3' end of each cDNA
873 fragment to guide the ligation of specific adapters. Adapters consisted of primers for
874 transcription and a specific index to code each sample. Samples were enriched with
875 limited-cycle PCR and analyzed to confirm the success of sample preparation before
876 sequencing using the Illumina© HiScanSQ platform available at the Multiusers Center
877 of Agricultural Biotechnology at the Department of Animal Sciences, ESALQ/USP.

878

879 **4.5. *De novo* transcriptome assembly**

880 Reads quality were visualized in FastQC software (Andrews, 2010) before
881 adapters removal and quality filtering by trimming the leading (LEADING:3) and
882 trailing (TRAILING:3) nucleotides until the quality was higher than 3, and then using a
883 sliding window of 4 nucleotides and trimming when scores were lower than 22
884 (SLIDINGWINDOW 4:22). Quality filtering was done using Trimmomatic-0.36
885 (Bolger et al., 2014).

886 All reads obtained were used to assemble a *de novo* transcriptome using the
887 pipeline available in the Trinity-v.2.4.0 software (Haas et al., 2013). Both paired and
888 unpaired trimmed and quality-filtered reads were used to assemble the *de novo*
889 transcriptome, which was further used as the reference transcriptome for the RNA-Seq
890 experiments. Assemblage was obtained using normalization of the reads coverage (<50)
891 and the minimum contig size selected was 200 nucleotides.

892 The transcripts obtained were functionally annotated using the BlastX algorithm
893 for putative identification of homologous sequences, with an *e*-value cut-off < 10⁻³.
894 Annotated sequences were curated and grouped into categories according to their

895 function using Blast2Go® (Conesa et al., 2005) with an *e*-value cut-off < 10⁻⁶ and
896 EggNOG-mapper 4.5.1 (Huerta-Cepas et al., 2017). Transcripts putatively identified as
897 belonging to insects and *Ca. L. asiaticus* were checked against the KEGG database
898 (Kyoto Encyclopedia of Genes and Genomes) (Kanehisa & Goto, 2000) to verify the
899 metabolic pathways represented in the obtained *de novo* transcriptome. Transcripts of
900 *Diaphorina citri*, *Ca. Liberibacter* spp. and *Wolbachia* spp. were filtered using Blast2go
901 version Pro (Götz et al. 2008).

902

903 **4.6. Differential gene expression analyses**

904 Changes in the pattern of gene expression were evaluated separately in gut of
905 ACP adults infected or not by *Ca. L. asiaticus* using the CLC Genomics Workbench
906 20.0 software (QIAGEN, Aarhus, Denmark). Reads from each library were counted
907 against the *de novo* transcriptome, and counts were normalized as transcripts per million
908 reads (TPM). TPM values for each sample were used to calculate fold-change ratios for
909 comparative analyses of the gene expression of control (CLas⁻) versus CLas-infected
910 insects (CLas⁺) within each feeding interval (1-2 d, 3-4 d, 5-6 d). Only the transcript
911 that were counted in two of the replicates of a particular treatment were further taken for
912 comparative analysis. Data were analyzed using multifactorial statistics based on a
913 negative binomial Generalized Linear Model (GLM). The values of fold change
914 obtained were corrected with False Discovery Rate (FDR) method and only transcripts
915 that showed *p*-value ≤0.05 and log fold change > |2| between treatments were
916 considered differentially expressed.

917

918 **Acknowledgements**

919 We are grateful to FAPESP for providing a post-doctoral fellowship to FMMB (grant:
920 2018/24234-4) and a research grant to FLC, NAW and LP to support this research
921 (grant: 15/07011-3). To CNPq for the PhD fellowship to JCD (grant: 141042/2017-6).
922 Authors also acknowledge the Fundecitrus support personnel team that provided the
923 required assistance for conducting this research.

924

925 **Author's contribution**

926 FLC and NAW designed the experiments; FLC, NAW and LP secured the funds; JCD
927 collected insect samples and extracted RNA; BLM processed the sequencing data and
928 assembled the *de novo* transcriptome; FMMB analyzed the data; FMMB and FLC wrote
929 the paper; all authors commented the initial draft and approved the final version of this
930 manuscript.

931

932 **References**

933

934 Abebe E, Gugsa G, Ahmed M. Review on Major Food-Borne Zoonotic Bacterial
935 Pathogens. *J Trop Med.* 2020;2020:4674235. doi: 10.1155/2020/4674235.

936

937 Agashe VR, Guha S, Chang HC, Genevaux P, Hayer-Hartl M, Stemp M, et al. Function
938 of trigger factor and DnaK in multidomain protein folding: increase in yield at the
939 expense of folding speed. *Cell.* 2004;117(2):199-209. doi: 10.1016/s0092-
940 8674(04)00299-5.

941

942 Ajene IJ, Khamis FM, van Asch B, Pietersen G, Seid N, Rwmushana I, et al.
943 Distribution of *Candidatus* Liberibacter species in Eastern Africa, and the First Report
944 of *Candidatus* Liberibacter asiaticus in Kenya. *Sci Rep.* 2020;10:3919. doi:
945 10.1038/s41598-020-60712-0.

946

947 Amherd R, Hintermann E, Walz D, Affolter M, Meyer UA. Purification, cloning, and
948 characterization of a second arylalkylamine N-acetyltransferase from *Drosophila*
949 *melanogaster*. *DNA Cell Biol.* 2000;19(11):697-705. doi:
950 10.1089/10445490050199081.

951

952 Ammar E, Shatters Jr RG, Lynch C, Hall DG. Detection and Relative Titer of
953 *Candidatus* Liberibacter asiaticus in the salivary glands and alimentary canal of
954 *Diaphorina citri* (Hemiptera: Psyllidae) vector of Citrus Huanglongbing Disease. *Ann*
955 *Entomol Soc Am.* 2011b;104(3):526-533. doi: 10.1603/AN10134.

956

957 Ammar E-D, Achor D, Levy A. Immuno-ultrastructural localization and putative
958 multiplication sites of Huanglongbing bacterium in Asian Citrus Psyllid *Diaphorina*
959 *citri*. *Insects.* 2019;10(12):422. doi: 10.3390/insects10120422.

960

961 Ammar E-D, George J, Sturgeon K, Stelinski LL, Shatters RG. Asian citrus psyllid
962 adults inoculate Huanglongbing bacterium more efficiently than nymphs when this
963 bacterium is acquired by early instar nymphs. *Sci Rep.* 2020;10(1)18244. doi:
964 10.1038/s41598-020-75249-5.

965

966 Ammar E-D, Hall DG, Shatters RG Jr. Ultrastructure of the salivary glands, alimentary
967 canal and bacteria-like organisms in the Asian citrus psyllid, vector of citrus
968 Huanglongbing disease bacteria. *J Microsc Ultrastruct*. 2017;5:9-20. doi:
969 10.1016/j.jmau.2016.01.005.

970

971 Ammar E-D, Ramos JE, Hall DG, Dawson WO, Shatters RG Jr. Acquisition, replication
972 and inoculation of *Candidatus* *Liberibacter asiaticus* following various acquisition
973 periods on Huanglongbing-Infected citrus by nymphs and adults of the Asian Citrus
974 Psyllid. *PLoS One*. 2016;11(7): e0159594. doi: 10.1371/journal.pone.0159594.

975

976 Ammar E-D, Shatters Jr RG, Hall DG. Localization of *Candidatus* *Liberibacter*
977 *asiaticus*, associated with Citrus Huanglongbing Disease, in its psyllid vector using
978 fluorescence in situ hybridization. *J Phytopathol*. 2011a;159:726-734. doi:
979 10.1111/j.1439-0434.2011.01836.x.

980

981 Anderson KV. Toll signaling pathways in the innate immune response. *Curr Opin*
982 *Immunol*. 2000;12(1):13-19. doi: 10.1016/s0952-7915(99)00045-x.

983

984 Andrade M, Li JY, Wang N. *Candidatus* *Liberibacter asiaticus*: virulence traits and
985 control strategies. *Trop Plant Pathol*. 2020b;45:285-297. doi: 10.1007/s40858-020-
986 00341-0.

987

988 Andrade M, Wang N. (2019) The Tad Pilus apparatus of ‘*Candidatus* *Liberibacter*
989 *asiaticus*’ and its regulation by VisNR. *Mol Plant Microbe Interact*. 2019;32(9):1175-
990 1187. doi: 10.1094/MPMI-02-19-0052-R.

991

992 Andrade MO, Pang Z, Achor DS, Wang H, Yao T, Singer BH, Wang N. The flagella of
993 ‘*Candidatus* *Liberibacter asiaticus*’ and its movement *in planta*. *Mol Plant Pathol*.
994 2020a;21:109-123. doi: 10.1111/mpp.12884.

995

996 Andrews S. FastQC: a quality control tool for high throughput sequence data [software].
997 2010 [cited 2021 Feb 26]. Available from:
998 <http://www.bioinformatics.babraham.ac.uk/projects/fastqc>.
999

1000 Bajgar A, Jindra M, Dolezel D. Autonomous regulation of the insect gut by circadian
1001 genes acting downstream of juvenile hormone signaling. *Proc Natl Acad Sci U S A*.
1002 2013;110(11):4416-4421. doi: 10.1073/pnas.1217060110.

1003 Bardy SL, Ng SYM, Jarrell KF. Prokaryotic motility structures. *Microbiology*.
1004 2003;149:295-304. doi: 10.1099/mic.0.25948-0.

1005

1006 Bassanezi RB, Lopes AS, Miranda MP, Wulff NA, Volpe HXL, Ayres, AJ. Overview
1007 of citrus huanglongbing spread and management strategies in Brazil. *Trop Plant Pathol*.
1008 2020;45:251-264. doi: 10.1007/s40858-020-00343-y.

1009

1010 Baumann P. Biology bacteriocyte-associated endosymbionts of plant sap-sucking
1011 insects. *Annu Rev Microbiol*. 2005;59:155-89. doi:
1012 10.1146/annurev.micro.59.030804.121041.

1013

1014 Beinert H. A tribute to sulfur. *Eur J Biochem*. 2000;267:5657–5664. doi:
1015 10.1046/j.1432-1327.2000.01637.x.

1016

1017 Bendix C, Lewis JD. The enemy within: phloem-limited pathogens. *Mol Plant Pathol*.
1018 2018 Jan;19(1):238-254. doi: 10.1111/mpp.12526.

1019

1020 Benguettat O, Jneid R, Soltys J, Loudhaief R, Brun-Barale A, Osman D, Gallet A. The
1021 DH31/CGRP enteroendocrine peptide triggers intestinal contractions favoring the
1022 elimination of opportunistic bacteria. *PLoS Pathog*. 2018;14(9):e1007279. doi:
1023 10.1371/journal.ppat.1007279.

1024

1025 Bhattacharyya S, Feferman L, Tobacman JK. Arylsulfatase B regulates versican
1026 expression by galectin-3 and AP-1 mediated transcriptional effects. *Oncogene*.
1027 2014;33(47):5467-5476. doi: 10.1038/onc.2013.483.

1028

1029 Bolger AM, Lohse M, Usadel B. Trimmomatic: a flexible trimmer for Illumina
1030 sequence data. *Bioinformatics*. 2014;30(15):2114-2120. doi:
1031 10.1093/bioinformatics/btu170.

1032

1033 Bové JM, Garnier M. Phloem-and xylem-restricted plant pathogenic bacteria. *Plant Sci.*
1034 2003;164:423-438. doi: 10.1016/S0168-9452(03)00033-5.

1035

1036 Bové JM. Huanglongbing: A destructive newly emerging, century-old disease of citrus.
1037 *J Plant Pathol.* 2006;88:7-37. doi: 10.4454/jpp.v88i1.828.

1038

1039 Brodbeck D, Amherd R, Callaerts P, Hintermann E, Meyer UA, Affolter M. Molecular
1040 and biochemical characterization of the aaNAT1 (Dat) locus in *Drosophila*
1041 *melanogaster*: differential expression of two gene products. *DNA Cell Biol.*
1042 1998;17(7):621-633. doi: 10.1089/dna.1998.17.621.

1043

1044 Brunner E, Peter O, Schweizer L, Basler K. *pangolin* encodes a Lef-1 homologue that
1045 acts downstream of Armadillo to transduce the Wingless signal in *Drosophila*. *Nature*.
1046 1997;385(6619):829-833. doi: 10.1038/385829a0.

1047

1048 Buchon N, Broderick NA, Lemaitre B. Gut homeostasis in a microbial world: insights
1049 from *Drosophila melanogaster*. *Nat Rev Microbiol.* 2013;11(9):615-26. doi:
1050 10.1038/nrmicro3074.

1051

1052 CABI/EPPO. *Candidatus Liberibacter asiaticus* [Distribution map]. 4th ed. Wallingford:
1053 CABI.; 2017.

1054

1055 Caccia S, Casartelli M, Tettamanti G. The amazing complexity of insect midgut cells:
1056 types, peculiarities, and functions. *Cell Tissue Res.* 2019;377(3):505-525. doi:
1057 10.1007/s00441-019-03076-w.

1058

1059 Carr S, Penfold CN, Bamfold V, James R, Hemmings AM. The structure of TolB, an
1060 essential component of the tol-dependent translocation system, and its protein-protein

1061 interaction with the translocation domain of colicin E9. *Structure*. 2000;8:57-66. doi:
1062 10.1016/S0969-2126(00)00079-4.

1063

1064 Celli J, Gorvel JP. Organelle robbery: *Brucella* interactions with the endoplasmic
1065 reticulum. *Curr Opin Microbiol*. 2004;7(1):93-97. doi: 10.1016/j.mib.2003.11.001.

1066

1067 Cerveny L, Straskova A, Dankova V, Hartlova A, Ceckova M, Staud F, Stulik J.
1068 Tetratricopeptide repeat motifs in the world of bacterial pathogens: role in virulence
1069 mechanisms. *Infect Immun*. 2013;81(3):629-635. doi: 10.1128/IAI.01035-12.

1070

1071 Cicero JM, Fisher TW, Qureshi JA, Stansly PA, Brown JK. Colonization and Intrusive
1072 Invasion of Potato Psyllid by '*Candidatus Liberibacter solanacearum*'. *Phytopathology*.
1073 2017;107(1):36-49. doi: 10.1094/PHYTO-03-16-0149-R.

1074

1075 Conesa A, Götz S, García-Gómez JM, Terol J, Talón M, Robles M. Blast2GO: a
1076 universal tool for annotation, visualization and analysis in functional genomics research.
1077 *Bioinformatics*. 2005;21(18):3674-3676. doi: 10.1093/bioinformatics/bti610.

1078

1079 Cordero JB, Stefanatos RK, Scopelliti A, Vidal M, Sansom OJ. Inducible progenitor-
1080 derived Wingless regulates adult midgut regeneration in *Drosophila*. *EMBO J*.
1081 2012;31(19):3901-3917. doi: 10.1038/emboj.2012.248.

1082

1083 Dala-Paula BM, Raithore S, Manthey JA, Baldwin EA, Zhao W et al. Active taste
1084 compounds in juice from oranges symptomatic for Huanglongbing (HLB) citrus
1085 greening disease. *LWT – Food Science Technology*. 2018;9:518-525. doi:
1086 10.1016/j.lwt.2018.01.083.

1087

1088 Dala-Paula BM, Plotto A, Bai J, Manthey JA, Baldwin EA, Ferrarezi RS, Gloria MBA.
1089 Effect of Huanglongbing or Greening Disease on Orange Juice Quality, a Review. *Front
1090 Plant Sci*. 2019;9:1976. doi: 10.3389/fpls.2018.01976.

1091

1092 Dohrman A, Miyata S, Gallup M, Li JD, Chapelin C, Coste A, et al. Mucin gene (MUC
1093 2 and MUC 5AC) upregulation by Gram-positive and Gram-negative bacteria. *Biochim
1094 Biophys Acta*. 1998;1406(3):251-259. doi: 10.1016/s0925-4439(98)00010-6.

1095

1096 Duan Q, Zhou M, Zhu L, Zhu G. Flagella and bacterial pathogenicity. *J Basic
1097 Microbiol*. 2013;53(1):1-8. doi: 10.1002/jobm.201100335.

1098

1099 Dupont L, Garcia I, Poggi MC, Alloing G, Mandon K, Le Rudulier D. The
1100 *Sinorhizobium meliloti* ABC transporter Cho is highly specific for choline and
1101 expressed in bacteroids from *Medicago sativa* nodules. *J Bacteriol*. 2004;186(18):5988-
1102 96. doi: 10.1128/JB.186.18.5988-5996.2004.

1103

1104 Erlandson MA, Toprak U, Hegedus DD. Role of the peritrophic matrix in insect-
1105 pathogen interactions. *J Insect Physiol*. 2019;117:103894. doi:
1106 10.1016/j.jinsphys.2019.103894.

1107

1108 Eshwar AK, Guldmann C, Oevermann A, Tasara T. Cold-Shock Domain Family
1109 Proteins (Csps) Are Involved in Regulation of Virulence, Cellular Aggregation, and
1110 Flagella-Based Motility in *Listeria monocytogenes*. *Front Cell Infect Microbiol*.
1111 2017;7:453. doi: 10.3389/fcimb.2017.00453.

1112

1113 Estrella MA, Du J, Chen L, Rath S, Prangley E, Chitrakar A, Aoki T, Schedl P,
1114 Rabinowitz J, Korenykh A. The metabolites NADP+ and NADPH are the targets of
1115 the circadian protein Nocturnin (Curled). *Nat Commun*. 2019;10(1):2367. doi:
1116 10.1038/s41467-019-10125-z.

1117

1118 Faggioni R, Feingold KR, Grunfeld C. Leptin regulation of the immune response and
1119 the immunodeficiency of malnutrition. *FASEB J*. 2001;15(14):2565-71. doi:
1120 10.1096/fj.01-0431rev.

1121

1122 Fauci AS. Infectious diseases: considerations for the 21st century. *Clin Infect Dis*.
1123 2001;32(5):675-85. doi: 10.1086/319235.

1124

1125 Fong JNC, Yildiz FH. Biofilm Matrix Proteins. *Microbiol Spectr.*
1126 2015;3(2):10.1128/microbiolspec.MB-0004-2014. doi: 10.1128/microbiolspec.MB-
1127 0004-2014.

1128

1129 Franz A, Shlyueva D, Brunner E, Stark A, Basler K. Probing the canonicity of the
1130 Wnt/Wingless signaling pathway. *PLoS Genet.* 2017;13(4):e1006700. doi:
1131 10.1371/journal.pgen.1006700.

1132

1133 Friedman JR, Dibenedetto JR, West M, Rowland AA, Voeltz GK. Endoplasmic
1134 reticulum-endosome contact increases as endosomes traffic and mature. *Mol Biol Cell.*
1135 2013;24(7):1030-1040. doi: 10.1091/mbc.E12-10-0733.

1136

1137 Fu S, Shao J, Zhou C, Hartung JS. Transcriptome analysis of sweet orange trees
1138 infected with '*Candidatus Liberibacter asiaticus*' and two strains of Citrus Tristeza
1139 Virus. *BMC Genomics.* 2016;17:349. doi: 10.1186/s12864-016-2663-9.

1140

1141 Galganski L, Urbanek MO, Krzyzosiak WJ. Nuclear speckles: molecular organization,
1142 biological function and role in disease. *Nucleic Acids Res.* 2017;45(18):10350-10368.
1143 doi: 10.1093/nar/gkx759.

1144

1145 Galluzzi L, Vitale I, Aaronson SA, Abrams JM, Adam D, Agostinis P, Alnemri ES, et
1146 al. Molecular mechanisms of cell death: recommendations of the Nomenclature
1147 Committee on Cell Death 2018. *Cell Death Differ.* 2018;25(3):486-541. doi:
1148 10.1038/s41418-017-0012-4.

1149

1150 García B, Merayo-Lloves J, Martin C, Alcalde I, Quirós LM, Vazquez F. Surface
1151 Proteoglycans as Mediators in Bacterial Pathogens Infections. *Front Microbiol.*
1152 2016;7:220. doi: 10.3389/fmicb.2016.00220.

1153

1154 Ghanim M, Achor D, Ghosh S, Kontsedalov S, Lebedev G, Levy A. '*Candidatus*
1155 *Liberibacter asiaticus*' accumulates inside endoplasmic reticulum associated vacuoles in
1156 the gut cells of *Diaphorina citri*. *Sci Rep.* 2017;7(1):16945. doi: 10.1038/s41598-017-
1157 16095-w.

1158

1159 Giltner CL, Nguyen Y, Burrows LL. Type IV pilin proteins: versatile molecular
1160 modules. *Microbiol Mol Biol Rev.* 2012;76(4):740-72. doi: 10.1128/MMBR.00035-12.

1161

1162 Girard C, Will CL, Peng J, Makarov EM, Kastner B, Lemm I, et al. Post-transcriptional
1163 spliceosomes are retained in nuclear speckles until splicing completion. *Nat Commun.*
1164 2012;3:994. doi: 10.1038/ncomms1998.

1165

1166 Götz S, García-Gómez JM, Terol J, Williams TD, Nagaraj SH, Nueda MJ, et al. High-
1167 throughput functional annotation and data mining with the Blast2GO suite. *Nucleic
1168 Acids Res.* 2008;36(10):3420-35. doi: 10.1093/nar/gkn176.

1169

1170 Graça JV, Douhan GW, Halbert SE, Keremane ML, Lee RF, Vidalakis G, Zhao H.
1171 Huanglongbing: An overview of a complex pathosystem ravaging the world's citrus. *J
1172 Integr Plant Biol.* 2016;58(4):373-87. doi: 10.1111/jipb.12437.

1173

1174 Granger E, McNee G, Allan V, Woodman P. The role of the cytoskeleton and molecular
1175 motors in endosomal dynamics. *Semin Cell Dev Biol.* 2014;31(100):20-9. doi:
1176 10.1016/j.semcdb.2014.04.011.

1177

1178 Gray S, Cilia M, Ghani M. Circulative, "nonpropagative" virus transmission: an
1179 orchestra of virus-, insect-, and plant-derived instruments. *Adv Virus Res.* 2014;89:141-
1180 199. doi: 10.1016/B978-0-12-800172-1.00004-5.

1181

1182 Green ER, Mecsas J. Bacterial Secretion Systems: An Overview. *Microbiol Spectr.*
1183 2016;4(1):10.1128/microbiolspec.VMBF-0012-2015. doi:
1184 10.1128/microbiolspec.VMBF-0012-2015.

1185

1186 Guo X, Roberts MR, Becker SM, Podd B, Zhang Y, Chua SC Jr, et al. Leptin signaling
1187 in intestinal epithelium mediates resistance to enteric infection by *Entamoeba
1188 histolytica*. *Mucosal Immunol.* 2011;4(3):294-303. doi: 10.1038/mi.2010.76.

1189

1190 Haas BJ, Papanicolaou A, Yassour M, Grabherr M, Blood PD, Bowden J, et al. *De novo*
1191 transcript sequence reconstruction from RNA-seq using the Trinity platform for
1192 reference generation and analysis. *Nat Protoc.* 2013;8(8):1494-512. doi:
1193 10.1038/nprot.2013.084.

1194

1195 Hammer TJ, Janzen DH, Hallwachs W, Jaffe SP, Fierer N. Caterpillars lack a resident
1196 gut microbiome. *Proc Natl Acad Sci U S A.* 2017;114(36):9641-9646. doi:
1197 10.1073/pnas.1707186114.

1198

1199 Hansson GC. Role of mucus layers in gut infection and inflammation. *Curr Opin*
1200 *Microbiol.* 2012;15(1):57-62. doi: 10.1016/j.mib.2011.11.002.

1201

1202 Helbig JH, König B, Knospe H, Bubert B, Yu C, Lück CP, et al. The PPIase active site
1203 of *Legionella pneumophila* Mip protein is involved in the infection of eukaryotic host
1204 cells. *Biol Chem.* 2003;384(1):125-37. doi: 10.1515/BC.2003.013. PMID: 12674506.

1205

1206 Hijaz F, Al-Rimawi F, Manthey JA, Killiny N. Phenolics, flavonoids and antioxidant
1207 capacities in Citrus species with different degree of tolerance to Huanglongbing. *Plant*
1208 *Signal Behav.* 2020 May 3;15(5):1752447. doi: 10.1080/15592324.2020.1752447.

1209

1210 Hijaz FM, Manthey JA, Folimonova SY, Davis CL, Jones SE, Reyes-De-Corcuera JI.
1211 An HPLC-MS characterization of the changes in sweet orange leaf metabolite profile
1212 following infection by the bacterial pathogen *Candidatus Liberibacter asiaticus*. *PLoS*
1213 *One.* 2013;8(11):e79485. doi: 10.1371/journal.pone.0079485.

1214

1215 Hiragaki S, Suzuki T, Mohamed AA, Takeda M. Structures and functions of insect
1216 arylalkylamine N-acetyltransferase (iaaNAT); a key enzyme for physiological and
1217 behavioral switch in arthropods. *Front Physiol.* 2015;6:113. doi:
1218 10.3389/fphys.2015.00113.

1219

1220 Hirokawa N. Kinesin and dynein superfamily proteins and the mechanism of organelle
1221 transport. *Science.* 1998;279(5350):519-526. doi: 10.1126/science.279.5350.519.

1222

1223 Holzbaur EL, Vallee RB. DYNEINS: molecular structure and cellular function. *Annu*
1224 *Rev Cell Biol*. 1994;10:339-372. doi: 10.1146/annurev.cb.10.110194.002011.

1225

1226 Hopkins AM, Walsh SV, Verkade P, Boquet P, Nusrat A. Constitutive activation of
1227 Rho proteins by CNF-1 influences tight junction structure and epithelial barrier
1228 function. *J Cell Sci*. 2003;116:725-742. doi: 10.1242/jcs.00300.

1229

1230 Huang W, Reyes-Caldas P, Mann M, Seifbarghi S, Kahn A, Almeida RPP, et al.
1231 Bacterial Vector-Borne Plant Diseases: Unanswered Questions and Future Directions.
1232 *Mol Plant*. 2020;13(10):1379-1393. doi: 10.1016/j.molp.2020.08.010.

1233

1234 Huerta-Cepas J, Forsslund K, Coelho LP, Szklarczyk D, Jensen LJ, von Mering C, Bork
1235 P. Fast Genome-Wide Functional Annotation through Orthology Assignment by
1236 eggNOG-Mapper. *Mol Biol Evol*. 2017;34(8):2115-2122. doi: 10.1093/molbev/msx148.

1237

1238 Hughes KL, Abshire ET, Goldstrohm AC. Regulatory roles of vertebrate Nocturnin:
1239 insights and remaining mysteries. *RNA Biol*. 2018;15(10):1255-1267. doi:
1240 10.1080/15476286.2018.1526541.

1241

1242 Ito T, Igaki T. Dissecting cellular senescence and SASP in Drosophila. *Inflamm Regen*.
1243 2016;36:25. doi: 10.1186/s41232-016-0031-4.

1244

1245 Jagoueix S, Bove JM, Garnier M. The phloem-limited bacterium of greening disease of
1246 citrus is a member of the alpha subdivision of the Proteobacteria. *Int J Syst Bacteriol*.
1247 1994;44(3):379-786. doi: 10.1099/00207713-44-3-379.

1248

1249 Jing T, Wang F, Qi F, Wang Z. Insect anal droplets contain diverse proteins related to
1250 gut homeostasis. *BMC Genomics*. 2018;19(1):784. doi: 10.1186/s12864-018-5182-z.

1251

1252 Kanehisa M, Goto S. KEGG: kyoto encyclopedia of genes and genomes. *Nucleic Acids*
1253 *Res*. 2000;28(1):27-30. doi: 10.1093/nar/28.1.27.

1254

1255 Kazmierczak BI, Schniederberend M, Jain R. Cross-regulation of *Pseudomonas* motility
1256 systems: the intimate relationship between flagella, pili and virulence. *Curr Opin*
1257 *Microbiol.* 2015;28:78-82. doi: 10.1016/j.mib.2015.07.017.

1258

1259 Kiefl J, Kohlenberg B, Hartmann A, Obst K, Paetz S, Krammer G, Trautzsch S.
1260 Investigation on key molecules of Huanglongbing (HLB)-induced orange juice off-
1261 flavor. *J Agric Food Chem.* 2018;66(10):2370-2377. doi: 10.1021/acs.jafc.7b00892.

1262

1263 Klein DC. Arylalkylamine N-acetyltransferase: "the Timezyme". *J Biol Chem.*
1264 2007;282(7):4233-4237. doi: 10.1074/jbc.R600036200.

1265

1266 Knoops B, Argyropoulou V, Becker S, Ferté L, Kuznetsova O. Multiple Roles of
1267 Peroxiredoxins in Inflammation. *Mol Cells.* 2016;39(1):60-4. doi:
1268 10.14348/molcells.2016.2341.

1269

1270 Kocks C. Intracellular motility. Profilin puts pathogens on the actin drive. *Curr Biol.*
1271 1994;4(5):465-8. doi: 10.1016/s0960-9822(00)00105-6.

1272

1273 Kodrík D, Bednářová A, Zemanová M, Krishnan N. Hormonal regulation of response to
1274 oxidative stress in insects-an update. *Int J Mol Sci.* 2015;16(10):25788-816. doi:
1275 10.3390/ijms161025788.

1276

1277 Kostygov AY, Frolov AO, Malysheva MN, Ganyukova AI, Chistyakova LV, Tashyreva
1278 D, et al. *Vickermania* gen. nov., trypanosomatids that use two joined flagella to resist
1279 midgut peristaltic flow within the fly host. *BMC Biol.* 2020;18(1):187. doi:
1280 10.1186/s12915-020-00916-y.

1281

1282 Kruse A, Fattah-Hosseini S, Saha S, Johnson R, Warwick E, Sturgeon K, et al.
1283 Combining 'omics and microscopy to visualize interactions between the Asian citrus
1284 psyllid vector and the Huanglongbing pathogen *Candidatus Liberibacter asiaticus* in the
1285 insect gut. *PLoS One.* 2017;12(6):e0179531. doi: 10.1371/journal.pone.0179531.

1286

1287 Kuraishi T, Binggeli O, Opota O, Buchon N, Lemaitre B. Genetic evidence for a
1288 protective role of the peritrophic matrix against intestinal bacterial infection in
1289 *Drosophila melanogaster*. Proc Natl Acad Sci U S A. 2011;108(38):15966-71. doi:
1290 10.1073/pnas.1105994108.

1291

1292 Lakhssassi N, Liu S, Bekal S, Zhou Z, Colantonio V, Lambert K, et al. Characterization
1293 of the Soluble NSF Attachment Protein gene family identifies two members involved in
1294 additive resistance to a plant pathogen. Sci Rep. 2017;7:45226. doi: 10.1038/srep45226.

1295

1296 Lamarche MG, Wanner BL, Crépin S, Harel J. The phosphate regulon and bacterial
1297 virulence: a regulatory network connecting phosphate homeostasis and pathogenesis.
1298 FEMS Microbiol Rev. 2008;32(3):461-73. doi: 10.1111/j.1574-6976.2008.00101.x.

1299

1300 Laothamatas I, Gao P, Wickramaratne A, Quintanilla CG, Dino A, Khan CA, Liou J,
1301 Green CB. Spatiotemporal regulation of NADP(H) phosphatase Nocturnin and its role
1302 in oxidative stress response. Proc Natl Acad Sci U S A. 2020;117(2):993-999. doi:
1303 10.1073/pnas.1913712117.

1304

1305 Layer G, Gaddam SA, Ayala-Castro CN, Ollagnier-de Choudens S, Lascoux D,
1306 Fontecave M, Outten FW. SufE transfers sulfur from SufS to SufB for iron-sulfur
1307 cluster assembly. J Biol Chem. 2007;282(18):13342-50. doi: 10.1074/jbc.M608555200.

1308

1309

1310 Lehane MJ, Billingsley PF. Biology of the Insect Midgut. Dordrecht:
1311 Springer Netherlands; 1996. doi : 10.1007/978-94-009-1519-0.

1312

1313 Li W, Hartung JS, Levy L. Quantitative real-time PCR for detection and identification
1314 of *Candidatus Liberibacter* species associated with citrus huanglongbing. J Microbiol
1315 Methods. 2006a;66(1):104-15. doi: 10.1016/j.mimet.2005.10.018.

1316

1317 Li Y, Park JS, Deng JH, Bai Y. Cytochrome c oxidase subunit IV is essential for
1318 assembly and respiratory function of the enzyme complex. J Bioenerg Biomembr.
1319 2006b;38(5-6):283-91. doi: 10.1007/s10863-006-9052-z.

1320

1321 Li W, Cong Q, Pei J, Kinch LN, Grishin NV. The ABC transporters in *Candidatus*
1322 *Liberibacter asiaticus*. *Proteins*. 2012;80(11):2614-28. doi: 10.1002/prot.24147.

1323

1324 Liu R, Ochman H. Origins of flagellar gene operons and secondary flagellar systems. *J*
1325 *Bacteriol*. 2007;189(19):7098-7104. doi: 10.1128/JB.00643-07.

1326

1327 Loftus SR, Walker D, Maté MJ, Bonsor DA, James R, Moore GR, Kleanthous C.
1328 Competitive recruitment of the periplasmic translocation portal TolB by a natively
1329 disordered domain of colicin E9. *Proc Natl Acad Sci U S A*. 2006;103(33):12353-8.
1330 doi: 10.1073/pnas.0603433103.

1331

1332 Lu H, Zhu J, Yu J, Chen X, Kang L, Cui F. A Symbiotic Virus Facilitates Aphid
1333 Adaptation to Host Plants by Suppressing Jasmonic Acid Responses. *Mol Plant*
1334 *Microbe Interact*. 2020;33(1):55-65. doi: 10.1094/MPMI-01-19-0016-R.

1335

1336 Lu J, Holmgren A. The thioredoxin antioxidant system. *Free Radic Biol Med*.
1337 2014;66:75-87. doi: 10.1016/j.freeradbiomed.2013.07.036.

1338

1339 Lu ZJ, Huang YL, Yu HZ, Li NY, Xie YX, Zhang Q, et al. Silencing of the Chitin
1340 Synthase Gene Is Lethal to the Asian Citrus Psyllid, *Diaphorina citri*. *Int J Mol Sci*.
1341 2019a;20(15):3734. doi: 10.3390/ijms20153734.

1342

1343 Lu ZJ, Zhou CH, Yu HZ, Huang YL, Liu YX, Xie YX, et al. Potential roles of insect
1344 Tropomyosin1-X1 isoform in the process of *Candidatus* *Liberibacter asiaticus* infection
1345 of *Diaphorina citri*. *J Insect Physiol*. 2019b;114:125-135. doi:
1346 10.1016/j.jinsphys.2019.02.012.

1347

1348 Mackey-Lawrence NM, Petri WA Jr. Leptin and mucosal immunity. *Mucosal Immunol*.
1349 2012;5(5):472-9. doi: 10.1038/mi.2012.40.

1350

1351 Macnab RM. How bacteria assemble flagella. *Annu Rev Microbiol*. 2003;57:77-100.
1352 doi: 10.1146/annurev.micro.57.030502.090832.

1353

1354 Manjunath KL, Halbert SE, Ramadugu C, Webb S, Lee RF. Detection of '*Candidatus*
1355 *Liberibacter asiaticus*' in *Diaphorina citri* and its importance in the management of
1356 citrus huanglongbing in Florida. *Phytopathology*. 2008;98(4):387-396. doi:
1357 10.1094/PHYTO-98-4-0387.

1358

1359 Mansfield J, Genin S, Magori S, Citovsky V, Sriariyanum M, Ronald P, et al. Top 10
1360 plant pathogenic bacteria in molecular plant pathology. *Mol Plant Pathol*.
1361 2012;13(6):614-29. doi: 10.1111/j.1364-3703.2012.00804.x.

1362

1363 Massenti R, Lo Bianco R, Sandhu AK, Gu L, Sims C. Huanglongbing modifies quality
1364 components and flavonoid content of 'Valencia' oranges. *J Sci Food Agric*.
1365 2016;96(1):73-78. doi: 10.1002/jsfa.7061.

1366

1367 Matilla MA, Krell T. The effect of bacterial chemotaxis on host infection and
1368 pathogenicity. *FEMS Microbiol Rev*. 2018;42(1). doi: 10.1093/femsre/fux052.

1369

1370 Matsuoka Y, Li X, Bennett V. Adducin: structure, function and regulation. *Cell Mol
1371 Life Sci*. 2000;57(6):884-895. doi: 10.1007/PL00000731.

1372

1373 Mauck KE, Chesnais Q, Shapiro LR. Evolutionary Determinants of Host and Vector
1374 Manipulation by Plant Viruses. *Adv Virus Res*. 2018;101:189-250. doi:
1375 10.1016/bs.aivir.2018.02.007.

1376

1377 McFarland L, Francetić O, Kumamoto CA. A mutation of *Escherichia coli* SecA
1378 protein that partially compensates for the absence of SecB. *J Bacteriol*.
1379 1993;175(8):2255-2262. doi: 10.1128/jb.175.8.2255-2262.1993.

1380

1381 Melcarne C, Lemaitre B, Kurant E. Phagocytosis in Drosophila: From molecules and
1382 cellular machinery to physiology. *Insect Biochem Mol Biol*. 2019;109:1-12. doi:
1383 10.1016/j.ibmb.2019.04.002.

1384

1385 Merz F, Hoffmann A, Rutkowska A, Zachmann-Brand B, Bukau B, Deuerling E. The
1386 C-terminal domain of *Escherichia coli* trigger factor represents the central module of its
1387 chaperone activity. *J Biol Chem.* 2006;281(42):31963-31971. doi:
1388 10.1074/jbc.M605164200.

1389

1390 Moens S, Vanderleyden J. Functions of bacterial flagella. *Crit Rev Microbiol.*
1391 1996;22(2):67-100. doi: 10.3109/10408419609106456.

1392

1393 Molki B, Thi Ha P, Mohamed A, Killiny N, Gang DR, Omsland A, Beyenal H.
1394 Physiochemical changes mediated by "*Candidatus Liberibacter asiaticus*" in Asian
1395 citrus psyllids. *Sci Rep.* 2019;9(1):16375. doi: 10.1038/s41598-019-52692-7.

1396

1397 Moy RH, Cherry S. Antimicrobial autophagy: a conserved innate immune response in
1398 *Drosophila*. *J Innate Immun.* 2013;5(5):444-455. doi: 10.1159/000350326.

1399

1400 Münch D, Amdam GV, Wolschin F. Ageing in a eusocial insect: molecular and
1401 physiological characteristics of life span plasticity in the honey bee. *Funct Ecol.*
1402 2008;22(3):407-421. doi: 10.1111/j.1365-2435.2008.01419.x.

1403

1404 Nakhleh J, Moussawi LE, Osta MA. The melanization response in insect immunity.
1405 *Adv In Insect Phys.* 2017;52:83-109. doi: 10.1016/bs.aiip.2016.11.002.

1406

1407 Nardi JB, Miller LA, Bee CM. Interfaces between microbes and membranes of host
1408 epithelial cells in hemipteran midguts. *J Morphol.* 2019;280(7):1046-1060. doi:
1409 10.1002/jmor.21000.

1410

1411 Neish AS. Redox signaling mediated by the gut microbiota. *Free Radic Res.*
1412 2013;47(11):950-7. doi: 10.3109/10715762.2013.833331.

1413

1414 Norville IH, Breitbach K, Eske-Pogodda K, Harmer NJ, Sarkar-Tyson M, Titball RW,
1415 Steinmetz I. A novel FK-506-binding-like protein that lacks peptidyl-prolyl isomerase
1416 activity is involved in intracellular infection and in vivo virulence of *Burkholderia*
1417 *pseudomallei*. *Microbiology.* 2011;157:2629-2638. doi: 10.1099/mic.0.049163-0.

1418

1419 Pandey S, Tripathi D, Khubaib M, Kumar A, Sheikh JA, Sumanlatha G, Ehtesham NZ,
1420 Hasnain SE. *Mycobacterium tuberculosis* Peptidyl-Prolyl Isomerasases Are
1421 Immunogenic, Alter Cytokine Profile and Aid in Intracellular Survival. *Front Cell Infect*
1422 *Microbiol.* 2017;7:38. doi: 10.3389/fcimb.2017.00038.

1423

1424 Panz M, Vitos-Faleato J, Jendretzki A, Heinisch JJ, Paululat A, Meyer H. A novel role
1425 for the non-catalytic intracellular domain of Neprilysins in muscle physiology. *Biol*
1426 *Cell.* 2012;104(9):553-568. doi: 10.1111/boc.201100069.

1427

1428 Paone P, Cani PD. Mucus barrier, mucins and gut microbiota: the expected slimy
1429 partners? *Gut.* 2020;69(12):2232-2243. doi: 10.1136/gutjnl-2020-322260.

1430

1431 Perilla-Henao LM, Casteel CL. Vector-Borne Bacterial Plant Pathogens: Interactions
1432 with Hemipteran Insects and Plants. *Front Plant Sci.* 2016 Aug 9;7:1163. doi:
1433 10.3389/fpls.2016.01163.

1434

1435 Perkins A, Nelson KJ, Parsonage D, Poole LB, Karplus PA. Peroxiredoxins: guardians
1436 against oxidative stress and modulators of peroxide signaling. *Trends Biochem Sci.*
1437 2015;40(8):435-445. doi: 10.1016/j.tibs.2015.05.001.

1438

1439 Porter ME. Axonemal dyneins: assembly, organization, and regulation. *Curr Opin Cell*
1440 *Biol.* 1996;8(1):10-7. doi: 10.1016/s0955-0674(96)80042-1.

1441

1442 Prasad S, Xu J, Zhang Y, Wang N. SEC-Translocon Dependent Extracytoplasmic
1443 Proteins of *Candidatus* Liberibacter asiaticus. *Front Microbiol.* 2016;7:1989. doi:
1444 10.3389/fmicb.2016.01989.

1445

1446 Quigley EM. Gut bacteria in health and disease. *Gastroenterol Hepatol (N Y).*
1447 2013;9(9):560-9.

1448

1449 Quintana-Hayashi MP, Mahu M, De Pauw N, Boyen F, Pasmans F, Martel A, et al. The
1450 levels of *Brachyspira hyodysenteriae* binding to porcine colonic mucins differ between

1451 individuals, and binding is increased to mucins from infected pigs with *de novo*
1452 MUC5AC synthesis. *Infect Immun.* 2015;83(4):1610-9. doi: 10.1128/IAI.03073-14.

1453

1454 Rahman MM, Franch-Marro X, Maestro JL, Martin D, Casali A. Local Juvenile
1455 Hormone activity regulates gut homeostasis and tumor growth in adult *Drosophila*. *Sci*
1456 *Rep.* 2017;7(1):11677. doi: 10.1038/s41598-017-11199-9.

1457

1458 Ramsey JS, Chavez JD, Johnson R, Hosseinzadeh S, Mahoney JE, Mohr JP, et al.
1459 Protein interaction networks at the host-microbe interface in *Diaphorina citri*, the insect
1460 vector of the citrus greening pathogen. *R Soc Open Sci.* 2017;4(2):160545. doi:
1461 10.1098/rsos.160545.

1462

1463 Ramsey JS, Johnson RS, Hoki JS, Kruse A, Mahoney J, Hilf ME, et al. Metabolic
1464 Interplay between the Asian Citrus Psyllid and Its *Proftella* Symbiont: An Achilles'
1465 Heel of the Citrus Greening Insect Vector. *PLoS One.* 2015;10(11):e0140826. doi:
1466 10.1371/journal.pone.0140826.

1467

1468 Rasch J, Ünal CM, Klages A, Karsli Ü, Heinsohn N, Brouwer RMHJ, et al. Peptidyl-
1469 Prolyl-cis/trans-Isomerasases Mip and PpiB of *Legionella pneumophila* Contribute to
1470 Surface Translocation, Growth at Suboptimal Temperature, and Infection. *Infect*
1471 *Immun.* 2018;87(1):e00939-17. doi: 10.1128/IAI.00939-17.

1472

1473 Ray S, Da Costa R, Thakur S, Nandi D. *Salmonella* Typhimurium encoded cold shock
1474 protein E is essential for motility and biofilm formation. *Microbiology.*
1475 2020;166(5):460-473. doi: 10.1099/mic.0.000900.

1476

1477 Redder P, Hausmann S, Khemici V, Yasrebi H, Linder P. Bacterial versatility requires
1478 DEAD-box RNA helicases. *FEMS Microbiol Rev.* 2015;39(3):392-412. doi:
1479 10.1093/femsre/fuv011.

1480

1481 Riddell CE, Lobaton Garces JD, Adams S, Baribeau SM, Twell D, Mallon EB.
1482 Differential gene expression and alternative splicing in insect immune specificity. *BMC*
1483 *Genomics.* 2014;15(1):1031. doi: 10.1186/1471-2164-15-1031.

1484

1485 Roberts IS. The biochemistry and genetics of capsular polysaccharide production in
1486 bacteria. *Annu Rev Microbiol.* 1996;50:285-315. doi: 10.1146/annurev.micro.50.1.285.

1487

1488 Robinson CG, Roy CR. Attachment and fusion of endoplasmic reticulum with vacuoles
1489 containing *Legionella pneumophila*. *Cell Microbiol.* 2006;8(5):793-805. doi:
1490 10.1111/j.1462-5822.2005.00666.x.

1491

1492 Roche B, Aussel L, Ezraty B, Mandin P, Py B, Barras F. Iron/sulfur proteins biogenesis
1493 in prokaryotes: formation, regulation and diversity. *Biochim Biophys Acta.*
1494 2013;1827(3):455-469. doi: 10.1016/j.bbabi.2012.12.010.

1495

1496 Rothman JE. Mechanisms of intracellular protein transport. *Nature.* 1994;372(6501):55-
1497 63. doi: 10.1038/372055a0.

1498

1499 Santos CA, Janissen R, Toledo MA, Beloti LL, Azzoni AR, Cotta MA, Souza AP.
1500 Characterization of the TolB-Pal trans-envelope complex from *Xylella fastidiosa* reveals
1501 a dynamic and coordinated protein expression profile during the biofilm development
1502 process. *Biochim Biophys Acta.* 2015;1854:1372-1381. doi:
1503 10.1016/j.bbapap.2015.05.018.

1504

1505 Santos-Beneit F. The Pho regulon: a huge regulatory network in bacteria. *Front
1506 Microbiol.* 2015;6:402. doi: 10.3389/fmicb.2015.00402.

1507

1508 Santos-Ortega Y, Killiny N. Silencing of sucrose hydrolase causes nymph mortality and
1509 disturbs adult osmotic homeostasis in *Diaphorina citri* (Hemiptera: Liviidae). *Insect
1510 Biochem Mol Biol.* 2018;101:131-143. doi: 10.1016/j.ibmb.2018.09.003.

1511

1512 Schroeder BO. Fight them or feed them: how the intestinal mucus layer manages the gut
1513 microbiota. *Gastroenterol Rep (Oxf).* 2019;7(1):3-12. doi: 10.1093/gastro/goy052.

1514

1515 Shears SB, Hayakawa Y. Functional Multiplicity of an Insect Cytokine Family Assists
1516 Defense Against Environmental Stress. *Front Physiol.* 2019;10:222. doi:
1517 10.3389/fphys.2019.00222.

1518

1519 Silva CP, Silva JR, Vasconcelos FF, Petretski MD, Damatta RA, Ribeiro AF, Terra
1520 WR. Occurrence of midgut perimicrovillar membranes in paraneopteran insect orders
1521 with comments on their function and evolutionary significance. *Arthropod Struct Dev.*
1522 2004;33(2):139-148. doi: 10.1016/j.asd.2003.12.002.

1523

1524 Singerman A, Rogers ME. The economic challenges of dealing with citrus greening: the
1525 case of Florida. *J Integr Pest Manag.* 2020;11(1):1-7. doi: 10.1093/jipm/pnz037.

1526

1527 Solari P, Rivelli N, De Rose F, Picciau L, Murru L, Stoffolano JG Jr, Liscia A. Opposite
1528 effects of 5-HT/AKH and octopamine on the crop contractions in adult *Drosophila*
1529 *melanogaster*: Evidence of a double brain-gut serotonergic circuitry. *PLoS One.*
1530 2017;12(3):e0174172. doi: 10.1371/journal.pone.0174172.

1531 ~~Section 4: Lipids and Phospholipid Metabolism~~

1532

1533 Sohlenkamp C, López-Lara IM, Geiger O. Biosynthesis of phosphatidylcholine in
1534 bacteria. *Prog Lipid Res.* 2003;42(2):115-62. doi: 10.1016/s0163-7827(02)00050-4.

1535

1536

1537

1538

1539

1540 Stenbeck G. Soluble NSF-attachment proteins. *Int J Biochem Cell Biol.*
1541 1998;30(5):573-7. doi: 10.1016/s1357-2725(97)00064-2.

1542

1543 Stokes BA, Yadav S, Shokal U, Smith LC, Eleftherianos I. Bacterial and fungal pattern
1544 recognition receptors in homologous innate signaling pathways of insects and
1545 mammals. *Front Microbiol.* 2015;6:19. doi: 10.3389/fmicb.2015.00019.

1546

1547 Strand M, Micchelli CA. Quiescent gastric stem cells maintain the adult *Drosophila*
1548 stomach. *Proc Natl Acad Sci U S A.* 2011;108(43):17696-701. doi:
1549 10.1073/pnas.1109794108.

1550

1551 Thapa SP, De Francesco A, Trinh J, Gurung FB, Pang Z, Vidalakis G, Wang N, Ancona
1552 V, Ma W, Coaker G. Genome-wide analyses of *Liberibacter* species provides insights

1553 into evolution, phylogenetic relationships, and virulence factors. *Mol Plant Pathol.*
1554 2020;21(5):716-731. doi: 10.1111/mpp.12925.

1555

1556 Theodorou MC, Theodorou EC, Kyriakidis DA. Involvement of AtoSC two-component
1557 system in *Escherichia coli* flagellar regulon. *Amino Acids.* 2012;43(2):833-844. doi:
1558 10.1007/s00726-011-1140-7.

1559

1560 Tjota M, Lee SK, Wu J, Williams JA, Khanna MR, Thomas GH. Annexin B9 binds to
1561 β (H)-spectrin and is required for multivesicular body function in *Drosophila*. *J Cell Sci.*
1562 2011;124:2914-2926. doi: 10.1242/jcs.078667.

1563

1564 Tomaseto AF, Marques RN, Fereres A, Zanardi OZ, Volpe HXL, Alquézar B, Peña L,
1565 Miranda MP. Orange jasmine as a trap crop to control *Diaphorina citri*. *Sci Rep.*
1566 2019;9(1):2070. doi: 10.1038/s41598-019-38597-5.

1567

1568 Treutter D. Significance of flavonoids in plant resistance: a review. *Environ Chem Lett.*
1569 2006;4:147-157. doi: 10.1007/s10311-006-0068-8.

1570

1571 Turner AJ, Isaac RE, Coates D. The neprilysin (NEP) family of zinc
1572 metalloendopeptidases: genomics and function. *Bioessays.* 2001;23(3):261-269. doi:
1573 10.1002/1521-1878(200103)23:3<261::AID-BIES1036>3.0.CO;2-K.

1574

1575 Vallet-Gely I, Lemaitre B, Boccard F. Bacterial strategies to overcome insect defences.
1576 *Nat Rev Microbiol.* 2008;6(4):302-313. doi: 10.1038/nrmicro1870.

1577

1578 Vande Velde C, Cizeau J, Dubik D, Alimonti J, Brown T, Israels S, et al. BNIP3 and
1579 genetic control of necrosis-like cell death through the mitochondrial permeability
1580 transition pore. *Mol Cell Biol.* 2000;20(15):5454-5468. doi: 10.1128/mcb.20.15.5454-
1581 5468.2000.

1582

1583 Wang C, Chen Y, Zhou H, Li X, Tan Z. Adaptation mechanisms of *Rhodococcus* sp.
1584 CNS16 under different temperature gradients: Physiological and transcriptome.
1585 *Chemosphere.* 2020;238:124571. doi: 10.1016/j.chemosphere.2019.124571.

1586

1587 Wang N, Pierson EA, Setubal JC, Xu J, Levy JG, Zhang Y, Li J, Rangel LT, Martins J

1588 Jr. The *Candidatus* Liberibacter-Host Interface: Insights into Pathogenesis Mechanisms

1589 and Disease Control. *Annu Rev Phytopathol.* 2017;55:451-482. doi: 10.1146/annurev-

1590 phyto-080516-035513.

1591

1592 Webb BA, Strand MR, Dickey SE, Beck MH, Hilgarth RS, Barney WE, et al.

1593 Polydnavirus genomes reflect their dual roles as mutualists and pathogens. *Virology.*

1594 2006;347(1):160-74. doi: 10.1016/j.virol.2005.11.010.

1595

1596 Wegener C, Veenstra JA. Chemical identity, function and regulation of enteroendocrine

1597 peptides in insects. *Curr Opin Insect Sci.* 2015;11:8-13. doi:

1598 10.1016/j.cois.2015.07.003.

1599

1600 Weinbauer MG. Ecology of prokaryotic viruses. *FEMS Microbiol Rev.* 2004;28(2):127-

1601 81. doi: 10.1016/j.femsre.2003.08.001.

1602

1603 Witke W. The role of profilin complexes in cell motility and other cellular processes.

1604 *Trends Cell Biol.* 2004;14(8):461-469. doi: 10.1016/j.tcb.2004.07.003.

1605

1606 Wu K, Li S, Wang J, Ni Y, Huang W, Liu Q, Ling E. Peptide Hormones in the Insect

1607 Midgut. *Front Physiol.* 2020;11:191. doi: 10.3389/fphys.2020.00191.

1608

1609 Wu P, Sun P, Nie K, Zhu Y, Shi M, Xiao C, et al. A Gut Commensal Bacterium

1610 Promotes Mosquito Permissiveness to Arboviruses. *Cell Host Microbe.* 2019;25(1):101-

1611 112.e5. doi: 10.1016/j.chom.2018.11.004.

1612

1613 Wu SC, Liao CW, Pan RL, Juang JL. Infection-induced intestinal oxidative stress

1614 triggers organ-to-organ immunological communication in *Drosophila*. *Cell Host*

1615 *Microbe.* 2012;11(4):410-417. doi: 10.1016/j.chom.2012.03.004.

1616

1617 Wulff NA, Daniel B, Sassi RS, Moreira AS, Bassanezi RB, Sala I, et al. Incidence of
1618 *Diaphorina citri* Carrying *Candidatus Liberibacter asiaticus* in Brazil's Citrus Belt.
1619 Insects. 2020;11(10):672. doi: 10.3390/insects11100672.

1620

1621 Yu HZ, Li NY, Zeng XD, Song JC, Yu XD, Su HN, et al. Transcriptome Analyses of
1622 *Diaphorina citri* Midgut Responses to *Candidatus Liberibacter Asiaticus* Infection.
1623 Insects. 2020;11(3):171. doi: 10.3390/insects11030171.

1624

1625 Yu X, Killiny N. RNA interference-mediated control of Asian citrus psyllid, the vector
1626 of the huanglongbing bacterial pathogen. Trop Plant Pathol. 2020;45:298–305. doi:
1627 10.1007/s40858-020-00356-7.

1628

1629 Zalewska M, Kochman A, Estève JP, Lopez F, Chaoui K, Susini C, Ozyhar A,
1630 Kochman M. Juvenile hormone binding protein traffic - Interaction with ATP synthase
1631 and lipid transfer proteins. Biochim Biophys Acta. 2009;1788(9):1695-705. doi:
1632 10.1016/j.bbamem.2009.04.022.

1633

1634 Zhang B, Gong J, Zhang W, Xiao R, Liu J, Xu XZS. Brain-gut communications via
1635 distinct neuroendocrine signals bidirectionally regulate longevity in *C. elegans*. Genes
1636 Dev. 2018;32(3-4):258-270. doi: 10.1101/gad.309625.117.

1637

1638 Zhao M, Wang S, Li F, Dong D, Wu B. Arylsulfatase B Mediates the Sulfonation-
1639 Transport Interplay in Human Embryonic Kidney 293 Cells Overexpressing
1640 Sulfotransferase 1A3. Drug Metab Dispos. 2016;44(9):1441-1449. doi:
1641 10.1124/dmd.116.070938

1642

1643

1644

1645

1646

1647

1649 **S1 Table.** Differentially expressed CLas genes in the gut of *Diaphorina citri* adults
 1650 after 1-2 d (*A1CLas*⁺), 3-4 d (*A2CLas*⁺) and 5-6 d (*A3CLas*⁺) of infection by feeding on
 1651 CLas-infected citrus plants.

Comparison	Annotation	Transcript ID	FC	FDR
	2-octaprenyl-6-methoxyphenyl hydroxylase	DN14876_c0_g1_i1	13.9	0.02
	5-(carboxyamino)imidazole ribonucleotide synthase	DN14087_c0_g1_i2	12.6	0.03
	50S ribosomal protein L2	DN11710_c0_g1_i2	16.9	0.04
	AAA family ATPase	DN1679_c0_g1_i1	13.8	0.05
	alanine--tRNA ligase	DN14954_c0_g1_i1	17.2	0.01
	alpha/beta hydrolase	DN39212_c0_g1_i1	14.0	0.01
	amino acid ABC transporter permease	DN15630_c0_g2_i3	14.1	0.02
	argininosuccinate lyase	DN13884_c0_g1_i1	13.4	0.01
	aspartate aminotransferase	DN14989_c0_g1_i4	12.0	0.02
	aspartate aminotransferase family protein	DN11157_c0_g1_i1	13.9	0.03
	ATP-dependent protease ATPase subunit HslU	DN20210_c0_g3_i1	12.0	0.03
	beta-ketoacyl-ACP synthase I	DN14910_c0_g1_i1	13.8	0.04
	bifunctional glutamate N-acetyltransferase/amino-acid acetyltransferase ArgJ	DN10638_c0_g1_i1	14.6	0.03
	carbamoyl phosphate synthase small subunit	DN13724_c0_g1_i1	19.0	9.3e ⁻³
	Chloramphenicol-sensitive protein rarD	DN13473_c0_g1_i1	17.2	0.05
	chromosomal replication initiation protein	DN15038_c0_g1_i2	16.8	7.41e ⁻³
	cold-shock protein	DN10086_c0_g2_i1	20.0	0.02
	DEAD/DEAH box helicase	DN4052_c0_g1_i1	24.2	0.02
	DNA polymerase III subunit chi	DN12825_c0_g1_i1	11.2	0.04
	DNA topoisomerase I	DN14080_c0_g1_i1	11.9	0.04
	DNA topoisomerase IV subunit B	DN10717_c0_g1_i1	37.8	8.87e ⁻⁴
	DNA translocase FtsK	DN14450_c0_g1_i1	22.7	2.49e ⁻³
	DUF1874 domain-containing protein	DN14305_c0_g1_i1	31.4	9.46e ⁻⁴
	elongation factor G	DN17043_c0_g1_i1	14.2	0.05
	elongation factor P	DN12683_c0_g1_i1	31.9	0.01
	elongation factor Ts	DN14637_c0_g1_i1	11.1	0.04
	excinuclease ABC subunit C	DN45886_c0_g1_i1	14.8	0.03
	exodeoxyribonuclease VII large subunit	DN17192_c0_g4_i3	14.0	9.3e ⁻³
	exonuclease I	DN15585_c7_g1_i1	11.2	0.02
	fumarate hydratase	DN14954_c0_g1_i2	23.9	6.8e ⁻³
	glutaminase	DN14270_c0_g1_i1	13.0	0.03
	glutathione S-transferase	DN4544_c0_g1_i1	17.5	0.04
	glycerol kinase	DN16960_c2_g1_i14	34.4	0.01
	glycine/betaine ABC transporter substrate-binding protein	DN15178_c0_g1_i1	33.1	2.07e ⁻³

A1CLas*⁺ x **A3CLas*⁺

hypothetical protein	DN14113_c1_g1_i1	16.2	0.02
hypothetical protein	DN17456_c0_g1_i2	23.7	0.01
hypothetical protein	DN17456_c0_g1_i3	14.2	0.03
hypothetical protein	DN17456_c0_g1_i4	22.0	$3.66e^{-3}$
hypothetical protein	DN17456_c0_g2_i1	17.3	0.04
hypothetical protein CGUJ_01660	DN14113_c0_g2_i1	16.5	0.05
hypothetical protein DJ66_0664	DN16265_c0_g2_i2	30.5	$1.15e^{-3}$
IMP dehydrogenase	DN6964_c0_g2_i1	13.6	0.03
isocitrate dehydrogenase	DN15328_c0_g1_i1	13.5	0.06
leucyl aminopeptidase	DN13997_c0_g1_i1	34.9	0.02
LuxR family transcriptional regulator	DN14940_c0_g2_i1	11.9	0.05
molecular chaperone DnaK	DN15220_c0_g1_i1	28.2	0.01
molecular chaperone GroEL	DN14757_c0_g1_i1	20.2	0.03
N-acetyl-gamma-glutamyl-phosphate reductase	DN15330_c0_g1_i2	14.7	0.05
NADH dehydrogenase	DN15210_c0_g1_i2	14.4	0.03
NifU family protein	DN5715_c0_g1_i1	11.8	0.05
nitrate ABC transporter ATP-binding protein	DN14488_c0_g2_i1	12.8	0.03
orotidine 5'-phosphate decarboxylase/BAX inhibitor (BI)-1/YccA family protein	DN14873_c0_g1_i1	13.5	0.04
PAS domain-containing sensor histidine kinase	DN14346_c0_g1_i1	13.9	0.02
penicillin-binding protein	DN14783_c0_g1_i1	11.9	0.03
periplasmic solute binding protein	DN15099_c0_g1_i1	9.7	0.04
permease	DN13997_c0_g2_i1	14.8	0.03
peroxiredoxin	DN17546_c4_g1_i1	13.5	0.03
phage repressor protein	DN15458_c0_g2_i5	20.6	0.03
phosphopyruvate hydratase	DN14337_c0_g1_i1	9.4	0.03
phosphoribosylformylglycinamide cyclo-ligase	DN27217_c0_g1_i1	17.8	$4.73e^{-3}$
pilus assembly protein	DN13708_c0_g1_i2	10.8	0.03
poly(A) polymerase	DN12871_c0_g1_i1	11.9	0.05
porin	DN10141_c0_g1_i1	86.2	$5.55e^{-4}$
porin family protein	DN15690_c0_g1_i2	19.8	0.03
putative protease IV transmembrane protein	DN14809_c0_g1_i2	12.7	0.05
pyridoxine 5'-phosphate synthase	DN15414_c0_g1_i4	19.1	0.01
pyruvate kinase/carbamoyl phosphate synthase large subunit	DN15141_c0_g1_i1	15.8	0.04
replicative DNA helicase	DN15002_c0_g1_i2	20.9	0.03
response regulator	DN12200_c0_g1_i1	16.8	0.02
ribonuclease D	DN10298_c0_g1_i1	16.4	0.03
signal recognition particle protein	DN15243_c0_g1_i2	38.6	$1.17e^{-3}$
succinyl-diaminopimelate desuccinylase	DN14376_c0_g1_i1	12.7	0.03
sulfonate ABC transporter permease	DN15690_c0_g1_i1	10.2	0.03

**A2CLas⁺ x A3CLas⁺	TerC family protein	DN11390_c0_g1_i1	10.8	0.05
	tetratricopeptide repeat protein	DN14826_c0_g1_i2	16.4	$8.26e^{-3}$
	thioredoxin-dependent thiol peroxidase	DN10526_c0_g1_i1	10.8	0.05
	threonine--tRNA ligase	DN10111_c0_g1_i1	11.8	0.04
	thymidylate kinase	DN14879_c0_g1_i1	13.2	0.03
	TIGR02300 family protein	DN20462_c0_g8_i1	13.9	0.03
	translation initiation factor IF-3	DN14949_c0_g2_i1	14.6	0.03
	trigger factor	DN13945_c0_g1_i1	11.5	0.04
	tRNA(5-methylaminomethyl-2-thiouridylate)- methyltransferase	DN53941_c0_g1_i1	17.1	0.05
	tRNA-dihydrouridine synthase A	DN14326_c0_g1_i1	14.2	0.02
	two-component system sensor histidine kinase AtoS	DN14305_c0_g2_i1	20.4	0.04
	type I methionyl aminopeptidase	DN13945_c0_g2_i1	16.4	$7.51e^{-3}$
	ubiquinone biosynthesis protein UbiB	DN13521_c0_g1_i1	9.8	0.03
	3-oxoacyl-ACP synthase	DN17762_c4_g2_i2	36.8	$1.85e^{-3}$
	bordetella phage Bbp38 like protein	DN15458_c0_g2_i1	9.6	0.03
	cell wall-associated hydrolase	DN19816_c1_g6_i1	42.2	0.02
	Chloramphenicol-sensitive protein rarD	DN13473_c0_g1_i1	7.5	0.05
	DEAD/DEAH box helicase	DN4052_c0_g1_i1	9.7	0.02
	dicarboxylate/amino acid:cation symporter	DN14605_c0_g1_i1	7.0	0.04
	DNA topoisomerase IV subunit B	DN10717_c0_g1_i1	8.2	0.05
	ferrochelatase	DN15257_c0_g1_i1	7.0	0.01
	glycerol kinase	DN16085_c2_g1_i12	38.8	$2.50e^{-4}$
	glycerol kinase	DN16960_c2_g1_i14	24.0	$3.44e^{-3}$
	glycine/betaine ABC transporter substrate-binding protein	DN15178_c0_g1_i1	135.0	$3.57e^{-4}$
	helix-turn-helix transcriptional regulator	DN15227_c0_g1_i1	36.9	0.05
	HsdR family type I site-specific deoxyribonuclease	DN14127_c0_g1_i1	11.3	$5.14e^{-3}$
	hypothetical protein	DN10205_c0_g1_i1	13.1	0.02
	hypothetical protein	DN14146_c0_g1_i1	7.3	0.06
	hypothetical protein	DN17456_c0_g1_i4	7.1	0.02
	phage repressor protein/Prophage antirepressor	DN15458_c0_g2_i5	16.5	$5.14e^{-3}$
	phenylalanine--tRNA ligase subunit beta	DN14949_c0_g1_i2	19.9	0.02
	SAM-dependent methyltransferase	DN13350_c0_g1_i2	38.0	$2.35e^{-4}$
	threonine--tRNA ligase	DN10111_c0_g1_i1	8.9	0.01

1652

1653 *A1CLas⁺: adults that fed on CLas-infected citrus plant for 1-2 days;

1654 **A2CLas⁺: adults that fed on CLas-infected citrus plant for 3-4 days; and

1655 ***A3CLas⁺: adults that fed on CLas-infected citrus plant for 5-6 days.

1656

1657

1658 **Fig S1.** The analysis of the 248,850 contigs was conducted by Blast2Go, using Blastx to
1659 recover annotations with significant homology from the NCBI. All terms ‘Biological
1660 Processes’, ‘Molecular Function’ and ‘Cellular Component’ at level 2 are represented as
1661 percent over total number of sequences.

1662

1663 **Fig S2.** Distribution of alignments and transcripts of *de novo* assembly of *Diaphorina*
1664 *citri* gut that fed on healthy and CLas-infected citrus plant, after search for similarity in
1665 NCBI databank.

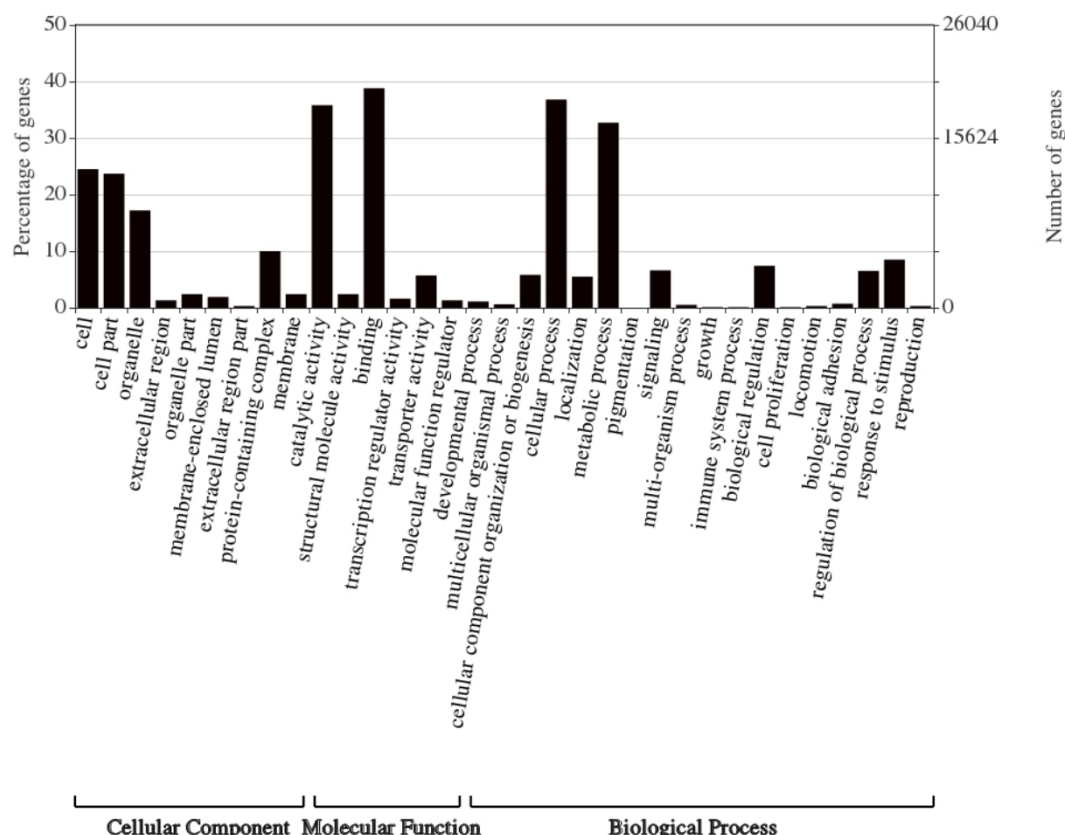
1666

1667 **Fig 1.** Venn diagram of *Candidatus Liberibacter asiaticus* transcripts differentially
1668 expressed in gut of adults at different periods of feeding on CLas-infected citrus plant.
1669 *A1CLas⁺*: adults that fed on CLas-infected citrus plant for 1-2 days; *A2CLas⁺*: adults
1670 that fed on CLas-infected citrus plant for 3-4 days; and *A3CLas⁺*: adults that fed on
1671 CLas-infected citrus plant for 5-6 days.

1672

1673 **Fig 2.** Venn diagram of *Diaphorina citri* transcripts differentially expressed in gut of
1674 adults at different periods of feeding on CLas-infected citrus plant compared to insects
1675 that fed on healthy citrus plant. A1 - *CLas⁺* x *CLas⁻*: adults that fed on CLas-infected
1676 versus uninfected citrus plant for 1-2 days; A2 - *CLas⁺* x *CLas⁻*: adults that fed on CLas-
1677 infected versus uninfected for 3-4 days; and A3 - *CLas⁺* x *CLas⁻*: adults that fed on
1678 CLas-infected versus uninfected for 5-6 days.

1679

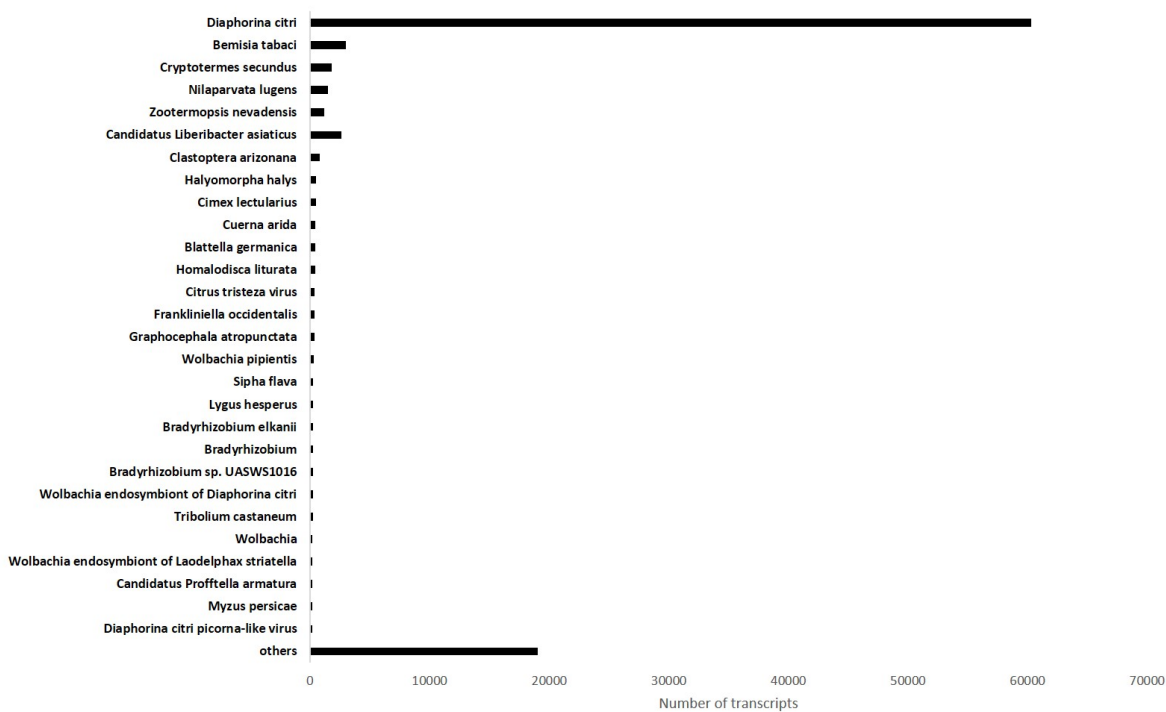


1680

1681

Fig S1.

1682



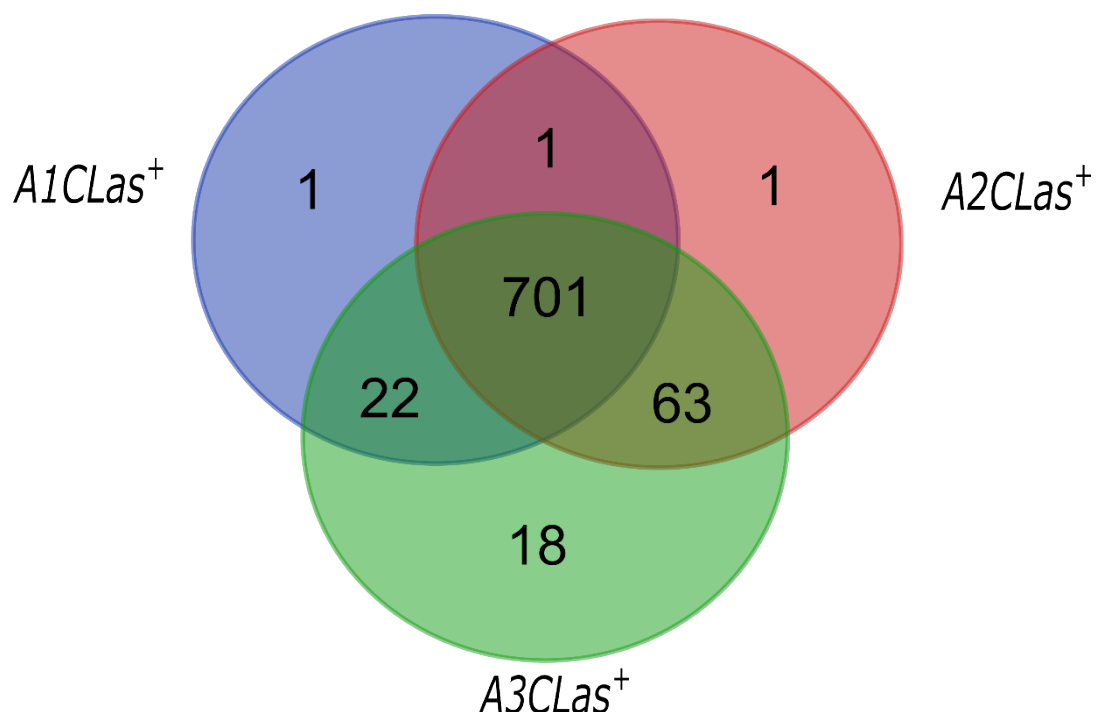
1683

1684 **Fig S2.**

1685

1686

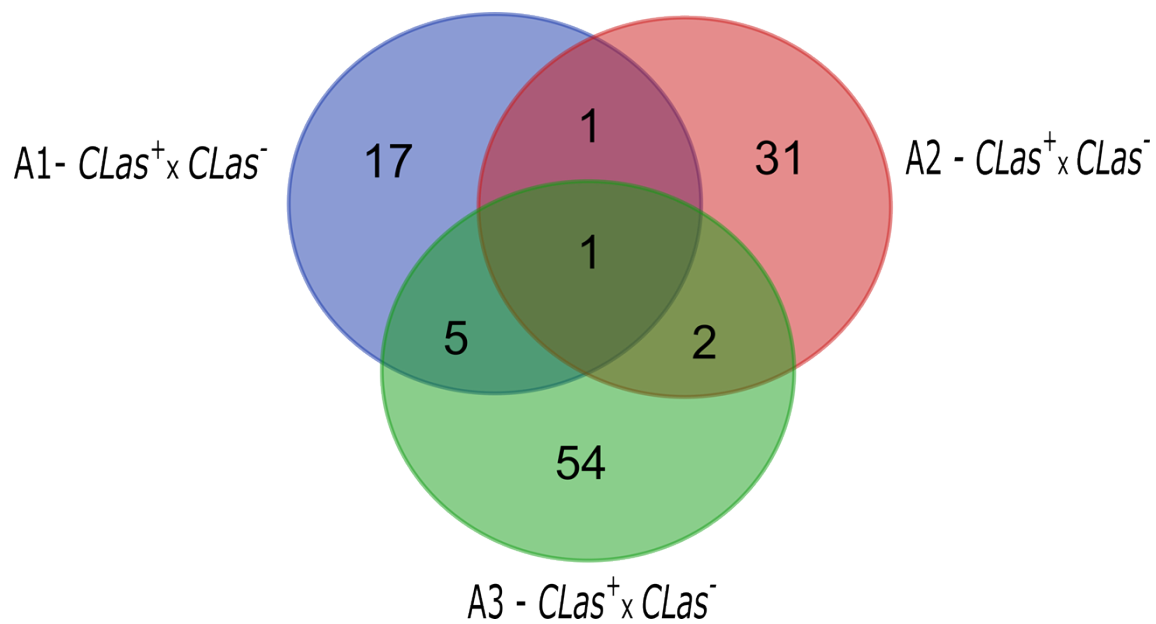
1687



1688

1689 **Fig 1.**

1690



1691

1692 **Fig 2.**

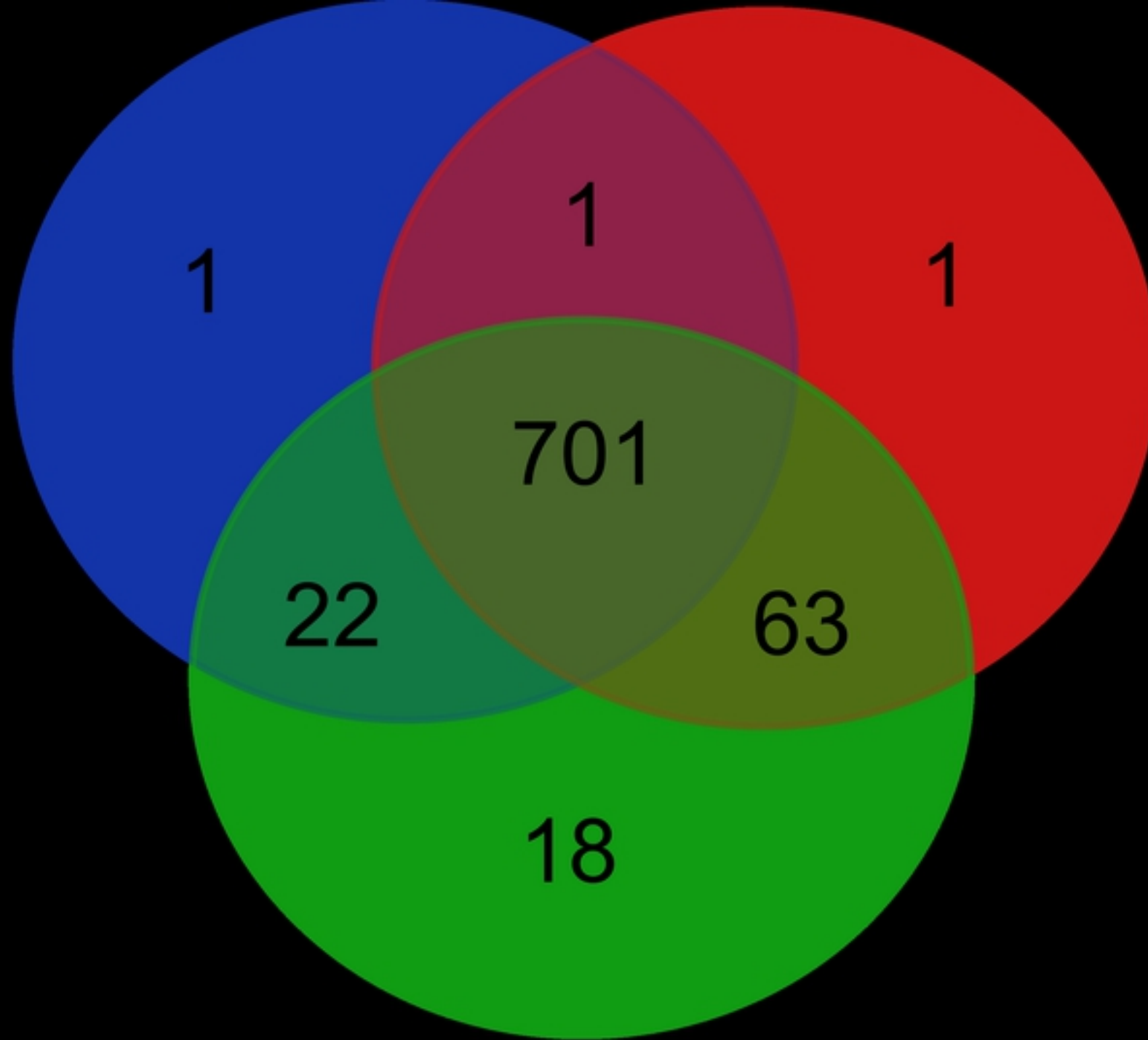


Figure 1

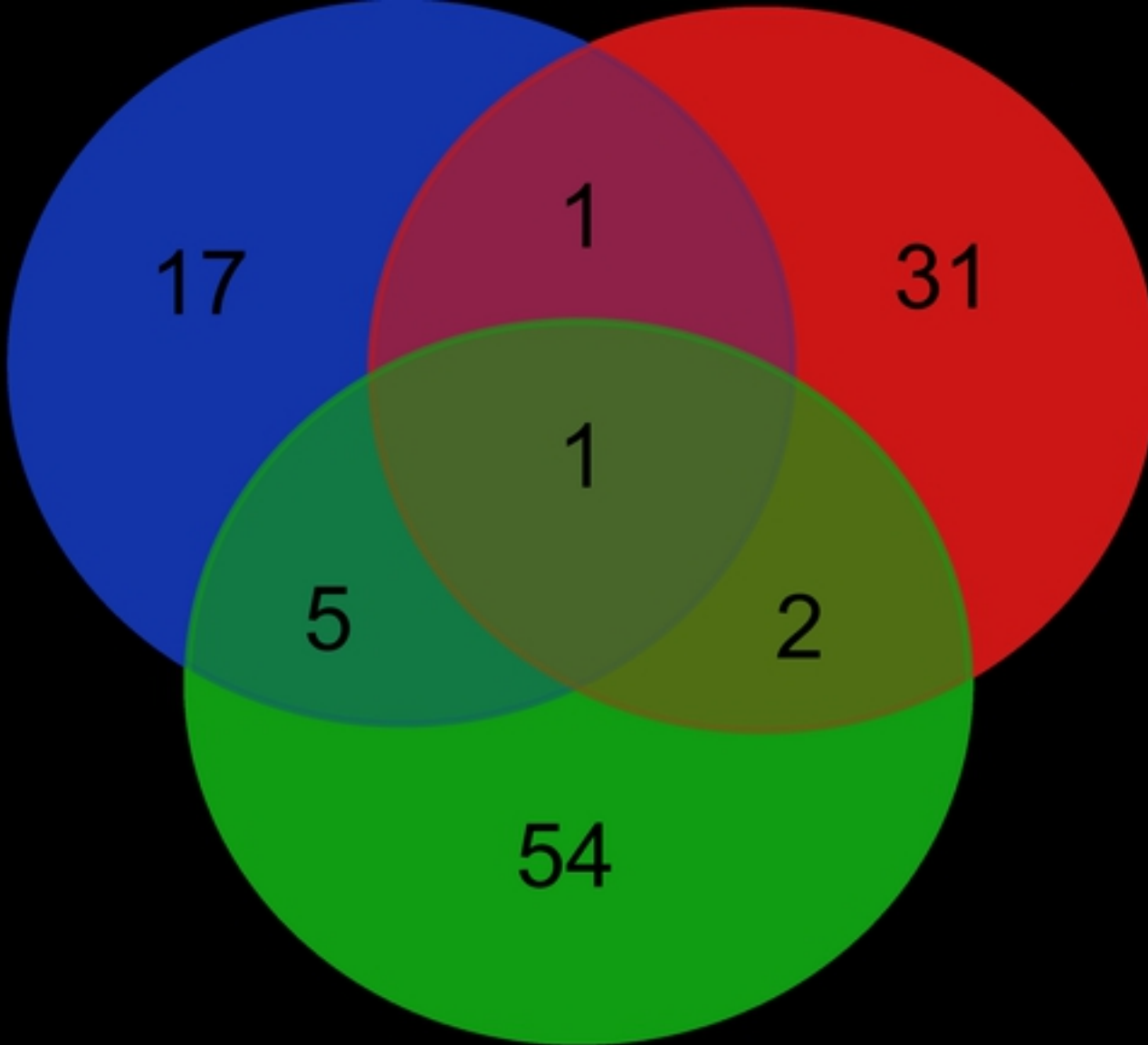


Figure 2